2011

# Modern Dirty Sea Ice Characteristics and Sources: The Role of Anchor Ice

Dennis A. Darby
*Old Dominion University*, ddarby@odu.edu

Wesley B. Myers
*Old Dominion University*

Martin Jakobsson

Ignatius Rigor



## Original Publication Citation

Darby, D. A., Myers, W. B., Jakobsson, M., & Rigor, I. (2011). Modern dirty sea ice characteristics and sources: The role of anchor ice. *Journal of Geophysical Research: Oceans, 116*, C09008. doi:10.1029/2010jc006675

# Modern dirty sea ice characteristics and sources: The role of anchor ice

Dennis A. Darby,[1] Wesley B. Myers,[1] Martin Jakobsson,[2] and Ignatius Rigor[3]

Received 23 September 2010; revised 18 May 2011; accepted 14 June 2011; published 13 September 2011.

[1] Extensive dirty ice patches with up to 7 kg $m^{-2}$ sediment concentrations in layers of up to 10 cm thickness were encountered in 2005 and 2007 in numerous areas across the central Arctic. The Fe grain fingerprint determination of sources for these sampled dirty ice floes indicated both Russian and Canadian sources, with the latter dominating. The presence of benthic shells and sea weeds along with thick layers (2–10 cm) of sediment covering 5–10 $m^2$ indicates an anchor ice entrainment origin as opposed to suspension freezing for some of these floes. The anchor ice origin might explain the dominance of Canadian sources where only narrow flaw leads occur that would not favor suspension freezing as an entrainment process. Expandable clays, commonly used as an indicator of a Kara Sea origin for dirty sea ice, are present in moderately high percentages (>20%) in many circum-Arctic source areas, including the Arctic coasts of North America. Some differences between the Russian and the North American coastal areas are found in clay mineral abundance, primarily the much higher abundance of chlorite in North America and the northern Barents Sea as opposed to the rest of the Russian Arctic. However, sea ice clay mineralogy matched many source areas, making it difficult to use as a provenance tool by itself. The bulk mineralogy (clay and non-clay) does not match specific sources possibly due to reworking of the sediment in dirty floes through summer melting or the failure to characterize all possible source areas.

**Citation:** Darby, D. A., W. B. Myers, M. Jakobsson, and I. Rigor (2011), Modern dirty sea ice characteristics and sources: The role of anchor ice, *J. Geophys. Res.*, *116*, C09008, doi:10.1029/2010JC006675.

## 1. Introduction

[2] The primary entrainment processes for sea ice were described 40 years ago [*Dayton et al.*, 1969; *Osterkamp and Gosink*, 1984; *Barnes et al.*, 1982] and while sea ice is one of the most important agents of sediment transport in the Arctic and polar seas, we still have little understanding of these processes and their relative importance. *Reimnitz et al.* [1998] included both the entrainment via frazil ice and anchor ice entrainment together as suspension freezing. However, with our current knowledge, these two entrainment processes should be separated because there are fundamental differences in the two and the conditions for each. Suspension freezing by frazil ice requires open water (normally winter polynya conditions) to allow for wave and tidal activity, bottom currents, or wind-driven Langmuir helical cells [*Gargett et al.*, 2004; *Dethleff and Kempema*, 2007; *Dethleff et al.*, 2009] to resuspend bottom sediment, whereby it is rafted to the surface by ice crystals forming near the bottom. This usually occurs in water depths of less than 50–60 m and mixing of subfreezing surface water to the bottom. We propose that the term suspension freezing be used for this process alone to avoid confusion with anchor ice entrainment. As *Reimnitz et al.* [1998] and earlier researchers correctly describe, the sediment in this frazil ice due to suspension freezing is dispersed throughout and is usually rather dilute and fine-grained with maximum sizes rarely exceeding 150 $\mu$m [*Barnes et al.*, 1982; *Kempema et al.*, 1989, 1993; *Reimnitz and Kempema*,1987]. On the other hand, anchor ice can form without open water and only requires freezing conditions at the bottom [*Reimnitz et al.*, 1987, 1992]. Anchor ice can still form throughout the winter without open water for waves and Langmuir cells to advect super-cooled surface water to depths of 30–60 m to freeze seawater near the bottom, if the bottom is frozen (permafrost) or seed ice crystals exist on the bottom.

[3] The observation of coastal polynyas coinciding with suspension freezing events has led to a general sense that this is the major process for entrainment and that by default, anchor ice is rare [*Eicken et al.*, 1997, 2005; *Stierle and Eicken*, 2002]. This paper looks at the two entrainment processes from a different approach. We will examine the dirty sea ice characteristics such as sediment concentration and sediment distribution in the ice, entrainment sources, and source area characteristics conducive to entrainment and then relate these to the processes of entrainment. We use two

[1]Department of Ocean, Earth, and Atmospheric Sciences, Old Dominion University, Norfolk, Virginia, USA.
[2]Department of Geological Sciences, Stockholm University, Stockholm, Sweden.
[3]Applied Physics Laboratory, University of Washington, Seattle, Washington, USA.


0148-0227/11/2010JC006675

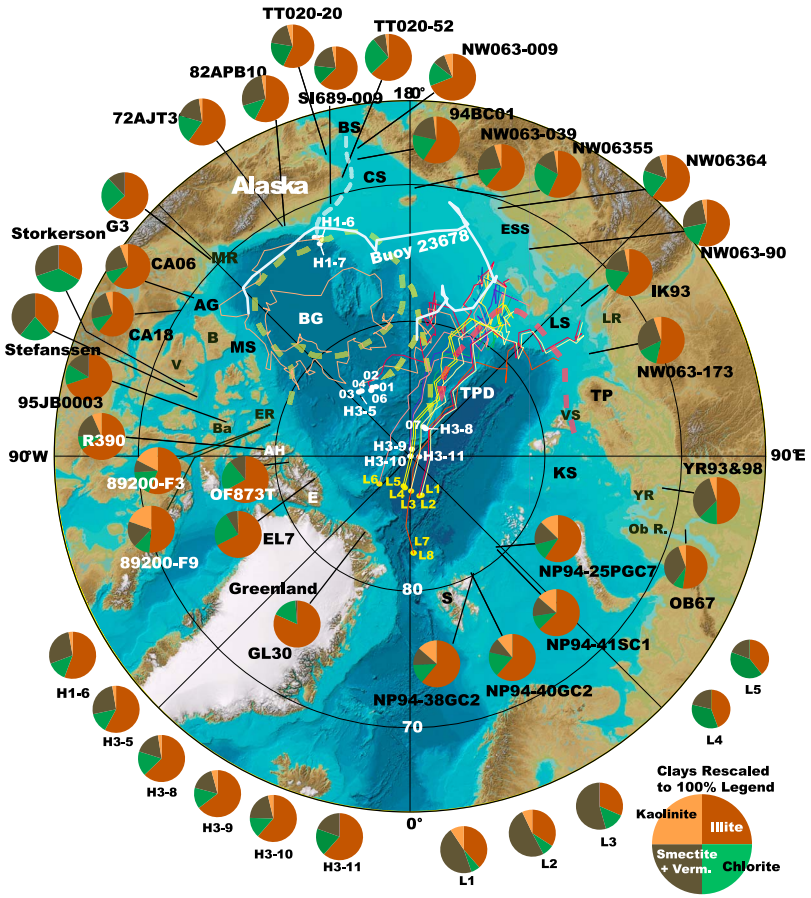


**Figure 1.** Location of dirty ice samples (H = HOTRAX expedition 2005 in white, L = LOMROG expedition 2007 in yellow), back trajectories for sea ice drift (solid lines) based on the date and location of each dirty ice sample; heavy white solid line is drift of buoy 23678 from near Banks Island on August 2003 to its position of last report in the central Arctic among the back trajectories of the HOTRAX dirty ice locations on September 2006; net drift paths based on buoy drift and circulation models (dashed lines after *Rigor and Wallace* [2004]) and these show the major drift patterns: BG = Beaufort Gyre and TPD = Trans Polar Drift; pie charts of clay mineral groups (Illite + muscovite, smectite + vermiculite + mixed layer expandable clays, chlorite, and kaolinite) rescaled to 100% from the bulk XRD mineralogy of the <45 $\mu$m size fraction from circum-Arctic source areas and dirty ice samples (below map). BS = Bering Strait, CS = Chukchi Sea, ESS = East Siberian Sea, LS = Laptev Sea, KS = Kara Sea, S = Svalbard, E = Ellesmere Island, AH = Axel Heiberg Island, ER = Ellef Ringnes Island, Ba = Bathurst Island, V = Victoria Island, B = Banks Island, MS = McClure Strait, AG = Amundsen Gulf, MR = Mackenzie R., LR = Lena R., VS = Vilkitski Strait, TP = Taymyr Peninsula, and YR = Yenisey R. The bathymetry is from the International Bathymetric Chart of the Arctic Ocean [*Jakobsson et al.*, 2008].

methods to determine the source of these dirty ice samples, the chemical fingerprint of individual Fe mineral grains and the clay/bulk mineralogy. As such we have expanded the analyses of circum-Arctic clay/bulk mineral data using some of the Fe grain source area samples for bulk X-Ray diffraction (XRD) determination of both clay and non-clay mineralogy.

[4] Sources of entrainment are important because if open water is required for suspension freezing, then areas will be favored where winter polynyas or flaw leads are common. If anchor ice is indicated as the mode of entrainment, then areas that would favor ice formation on the seafloor will be favored. These areas might be locations where permafrost conditions exist on or immediately below the seafloor, seed ice crystals form in the bottom sediment during fall freezeup, or where cold bottom waters allow low salinity water (possibly from groundwater where there is adequate precipitation or meltwater) to freeze in the pore spaces of bottom sediments.

## 2. Methods and Materials

[5] The Healy Oden Trans-Arctic Expedition (HOTRAX) in 2005 provided dirty sea ice samples from across the central Arctic as well as samples in the Beaufort Gyre near Alaska (Figure 1). In addition, the Lomonosov Ridge off Greenland (LOMROG) expedition in 2007 provided several more dirty ice samples from the area between Svalbard, the North Pole, and Greenland (Figure 1). Samples were collected from sediment concentrations and further concentrated

onboard to reduce meltwater. In most cases, this was accomplished by natural settling or partial drying. In a few cases samples were filtered through 0.45 $\mu$m filters using a vacuum pump or filtered through coffee filters for recovering Fe grains in the silt and sand fraction (~>45 $\mu$m).

[6] Randomly oriented powder mounts of the <45 $\mu$m fraction were prepared for X-ray diffraction (XRD). These samples (1 g) were mixed with 20% corundum as an internal standard and then ground in a McCrone micronizing mill with methanol to homogenize the samples [*Eberl*, 2003]. Random XRD mounts were prepared by side loading the sample against frosted glass to insure random orientation. These mounts were then analyzed on a Phillips X'pert Pro XRD system equipped with Cu-radiation from 5 to 65° 2$\theta$ with a step size of 0.02° $s^{-1}$. XRD patterns were then analyzed in the Excel macroprogram RockJock, to quantitatively determine the mineral constituents [*Eberl*, 2003]. This provided both the non-clay and clay mineralogy. Because nearly all previous studies used oriented mounts of the <2 $\mu$m fraction, several samples were run in this manner for comparison. For the oriented XRD runs, samples were first dispersed with Na metaphosphate and sonification and then the <2 $\mu$m separated by centrifugation. This size fraction was rapidly vacuum filtered onto 0.45 $\mu$m filters and then transferred onto glass slides by carefully rolling the filter onto the slide, allowing it to partially dry before removing the filter leaving the sample with the initial material sucked onto the filter exposed at the surface for XRD. This filter transfer method is preferred to avoid size segregation issues that can affect the proportions of different clay minerals, which tend to occur in different size fractions of the <2 $\mu$m clays. The mounts were heated at 70°C for 48 h minimum in a sealed container with ethylene glycol before XRD analyses from 3° to 30° 2$\theta$ to promote expansion of expandable clays The percentages of the four major clay groups (illite, smectite (expandable clays), chlorite, and kaolinite) were determined using mineral intensity ratios described by *Biscaye* [1965].

[7] Differences between the random mounted Rockjock XRD results and the oriented mounted methods are due to the fact that oriented mounts do not distinguish varieties of the same clay mineral group. In fact the mica minerals, biotite and muscovite will be included in the illite component when these minerals are <2 $\mu$m, which often occurs. Also vermiculite is often expandable and will thus be included in the smectite fraction of the oriented XRD results. Only several heat treatments of the oriented mounts can resolve this issue and these are rarely done. In order to minimize differences in the two methods, we included micas with illite and vermiculite with smectite in the sums and rescaled to 100% calculations (Figure 1 and Table 1).

[8] For the Fe oxide grain fingerprinting, the >45 $\mu$m fraction was separated from the dirty sea ice samples by wet-sieving at 250 $\mu$m, 63 $\mu$m, and 45 $\mu$m. The 45–63 and 63–250 $\mu$m fractions were dried and the magnetic minerals removed by hand magnet and then Frantz magnetic separation [*Darby*, 2003]. These two size fractions of magnetic separates were recombined and mounted in epoxy plugs, ground to expose the Fe oxide grains, polished, photographed, and the mineralogy of each of about 100 grains identified by reflected-light microscopy using 1000X oil-immersion. The grains were then analyzed by electron probe microanalysis (EPMA) for 12 elements [*Darby*, 2003]. These elements along with the mineralogy, which was subsequently checked against the composition for correctness, were used to match each grain to a source area from the circum-Arctic data set constructed earlier [*Darby and Bischof*, 1996; *Darby*, 2003]. The results are reported as weighted percents in order to avoid skewed percentages where low numbers of grains are matched to sources. Weighted percent is the percent of Fe grains matched to a particular source times the number of grains matched to this source divided by 10, a conservative number that exceeds the error of the matching procedure [*Darby*, 2003]. Thus 10 weighted percent equals 10 percent and weighted percentages below this are relatively diminished while those above are enhanced with values over 100 possible. This also reduces the effects of closure because the weighted percents from all sources do not sum to a constant.

[9] Size analyses were performed on bulk samples after several minutes of sonification with a horn sonifier at high intensity and the addition of Na-metaphosphate to maintain dispersion. Analyses were performed using a Malvern 2000 laser particle analyzer that detects sizes from 0.02 to 2000 $\mu$m [*Darby et al.*, 2009]. To determine the possible source areas for these samples, backward trajectories were estimated using monthly gridded fields of sea ice motion based on the observed drift from buoys, supplemented by retrievals of ice drift from satellites [*Rigor et al.*, 2002; *Maslanik et al.*, 1998].

## 3. Results

### 3.1. Field Observations

[10] All dirty sea ice samples taken in 2005 northwest of Barrow, Alaska, near the shelf edge consisted of small agglomerations (~1–4 mm) of sediment scattered throughout the ice in low concentrations. Only two of these samples contained more than a percent or two of sand (>63 $\mu$m) and thus very few Fe grains. The total sediment recovered at any of these sites ranged from 6 mg to 3 g. Generally less than half a square meter of surface area was sampled, so the sediment concentrations are up to 6 g $m^{-2}$. Because we did not collect a specific volume, we report values as g $m^{-2}$, but if we assume that nearly all of the sediment was collected from the ice for a given area, sample weights can be converted to g $m^{-3}$ for all estimations of sediment concentration. The highest sediment concentrations at the Alaskan sites is similar to concentrations found in the southern Kara Sea of 11 ± 25 g $m^{-3}$ [*Dethleff and Kuhlmann*, 2009] but far less than the 191.6 g $m^{-3}$ reported for a sea ice entrainment event near the New Siberian Islands and eastern Laptev Sea [*Eicken et al.*, 2000]. In contrast every dirty sea ice sample collected in the central Arctic in 2005/2007 was higher than 5 g and up to 1.8 kg. This upper limit is only a small fraction of what could have been collected from these sites because the dirty ice consisted of sediment layers covering 5–10 $m^2$ and represents sediment concentration at the ice surface down to 10 cm depth (Figures 2 and 3).

[11] Although 12 helicopter forays were conducted for dirty ice reconnaissance in the central Arctic during HOTRAX, most of the dirty ice spotted during this cruise was from the bridge of USCGC *Healy* and this may partly explain the higher concentrations of ice collected in

**Table 1.** XRD Results for the Circum-Arctic Source Samples and Dirty Ice Samples Using Both Bulk <45 $\mu$m (RockJock) and <2 $\mu$m [*Biscaye*, 1965] Quantitative Approaches[a]

| | Greenland GL30 | Ellesmere Is. EL7 | Otto Fiord OF-87-3-T | Axel Heiberg Is. R390 | Ellef Rignes Is. 89200 Avg[b] | Bathurst Is. 95BJB0003 | Victoria Is. Victoria Avg[b,c] | Amundsen Gulf CA06/18 Avg[b] |
|---|---|---|---|---|---|---|---|---|
| Minerals | | | | | | | | |
| Quartz | 32.8 | 23.5 | 28.6 | 24.2 | 27.8 | 22.2 | 4.6 | 21.7 |
| Kspar (ordered microcline) | 1.4 | 1.7 | 2.5 | 0.0 | 1.3 | 2.6 | 1.0 | 0.1 |
| Kspar (intermediate) | 0.0 | 0.0 | 0.4 | 0.8 | 2.3 | 1.0 | 0.0 | 2.3 |
| Kspar (Sanidine) | 0.4 | 0.0 | 0.0 | 0.5 | 0.4 | 1.9 | 0.4 | 0.5 |
| Kspar (orthoclase) | 0.2 | 0.2 | 0.6 | 1.4 | 0.3 | 1.0 | 0.0 | 0.5 |
| Kspar (anorthoclase) | 1.7 | 0.0 | 0.3 | 0.0 | 0.2 | 0.0 | 1.8 | 0.2 |
| Plag (Albite) | 8.1 | 5.2 | 0.2 | 4.4 | 2.6 | 4.4 | 5.6 | 2.9 |
| Plag (oligoclase) | 0.0 | 0.6 | 1.5 | 1.5 | 1.8 | 2.7 | 4.6 | 0.1 |
| Plag (Andesine) | 0.0 | 0.0 | 0.0 | 0.0 | 0.0 | 0.0 | 0.6 | 0.0 |
| Plag (Labradorite) | 0.0 | 0.0 | 0.2 | 0.0 | 0.7 | 0.0 | 0.2 | 0.0 |
| Plag (Bytownite) | 0.0 | 0.0 | 0.0 | 0.1 | 0.0 | 0.0 | 0.5 | 0.0 |
| Plag (Anorthite) | 0.9 | 0.1 | 0.0 | 0.0 | 1.4 | 0.0 | 2.6 | 0.0 |
| Calcite | 0.0 | 7.8 | 4.6 | 0.0 | 0.0 | 13.8 | 1.3 | 0.0 |
| Calcite (Mg-rich) | 0.0 | 0.0 | 0.0 | 0.0 | 0.0 | 0.0 | 0.0 | 0.0 |
| Dolomite | 0.3 | 7.5 | 32.3 | 1.0 | 0.8 | 8.7 | 59.8 | 8.1 |
| Amph. (Ferrot.) | 1.7 | 1.1 | 1.0 | 1.0 | 1.4 | 0.5 | 3.2 | 0.0 |
| Pyroxene (diopside) | 0.4 | 0.0 | 0.2 | 0.0 | 0.0 | 0.0 | 0.3 | 0.0 |
| Magnetite | 0.0 | 0.0 | 0.0 | 0.0 | 0.0 | 0.0 | 0.0 | 0.2 |
| Maghemite | 0.0 | 0.0 | 0.1 | 2.9 | 0.1 | 0.0 | 0.0 | 0.4 |
| Non-clays | 47.9 | 47.7 | 72.4 | 37.8 | 41.1 | 58.9 | 86.4 | 36.8 |
| | | | | | | | | |
| Kaolinite (disordered) | 0.0 | 0.0 | 0.0 | 3.3 | 9.4 | 0.0 | 0.0 | 3.3 |
| Kaolinite (dry branch) | 0.0 | 0.2 | 0.0 | 0.8 | 1.8 | 0.0 | 0.0 | 0.2 |
| Smectite (Na) | 0.0 | 0.0 | 0.0 | 2.5 | 0.0 | 0.0 | 0.0 | 0.2 |
| Smectite (Ca) | 0.0 | 1.0 | 0.1 | 0.5 | 4.2 | 0.0 | 0.0 | 4.5 |
| Smectite (hectorite) | 0.3 | 1.7 | 0.9 | 5.1 | 0.5 | 0.0 | 0.2 | 4.3 |
| Smectite (Fe) | 0.0 | 1.7 | 2.0 | 0.3 | 4.2 | 4.0 | 0.0 | 3.3 |
| Illite (1Md) | 2.3 | 0.8 | 3.9 | 15.2 | 12.5 | 11.0 | 0.0 | 16.8 |
| Illite (R > 1; 70–80%I) | 0.0 | 0.3 | 1.3 | 10.7 | 4.1 | 2.0 | 0.0 | 6.9 |
| Illite (RM30) | 0.0 | 4.1 | 3.9 | 2.1 | 1.7 | 1.0 | 0.0 | 0.8 |
| Biotite | 0.7 | 0.0 | 0.0 | 0.3 | 0.0 | 0.5 | 4.9 | 0.5 |
| Chlorite (Fe) | 6.7 | 9.2 | 6.1 | 5.1 | 6.9 | 5.1 | 4.0 | 4.8 |
| Chlorite (Mg) | 2.2 | 3.2 | 0.0 | 0.8 | 0.7 | 0.7 | 0.0 | 1.6 |
| Muscovite | 39.6 | 30.1 | 9.3 | 12.7 | 12.9 | 14.2 | 0.0 | 13.8 |
| Vermiculite | 0.3 | 0.0 | 0.0 | 3.0 | 0.0 | 2.6 | 4.5 | 2.3 |
| | | | | | | | | |
| Summed rescaled clays | | | | | | | | |
| Illite | 81.7 | 67.5 | 66.9 | 65.7 | 52.9 | 69.8 | 35.7 | 61.3 |
| Chlorite | 17.1 | 23.7 | 22.2 | 9.5 | 12.9 | 14.1 | 29.7 | 10.1 |
| Smectite | 1.2 | 8.4 | 10.9 | 18.2 | 15.1 | 16.1 | 34.6 | 23.0 |
| Kaolinite | 0.0 | 0.4 | 0.0 | 6.6 | 19.0 | 0.0 | 0.0 | 5.6 |
| | | | | | | | | |
| <2 $\mu$m filter transfers | | | | | | | | |
| Illite | 85.0 | 79.0 | 76.0 | 75.0 | | 77.5 | 74.0 | |
| Chlorite | 15.0 | 18.0 | 7.5 | 10.0 | | 11.0 | 13.0 | |
| Smectite | 0.0 | 0.5 | 9.0 | 5.0 | | 3.5 | 5.0 | |
| Kaolinite | 0.0 | 2.0 | 6.5 | 10.0 | | 8.0 | 8.0 | |
| | | | | | | | | |
| Difference RJ versus <2 $\mu$m | | | | | | | | |
| Illite | 3.3 | 11.5 | 9.1 | 9.3 | | 7.7 | 38.3 | |
| Chlorite | 2.1 | 5.7 | 14.7 | 0.5 | | 3.1 | 16.7 | |
| Smectite | 1.2 | 7.9 | 1.9 | 13.2 | | 12.6 | 29.6 | |
| Kaolinite | 0.0 | 1.6 | 6.5 | 3.4 | | 8.0 | 8.0 | |

[a]The summed clay groups from the RockJock calculations are plotted in Figure 1. The average error in absolute percent between the two methods for the summed clays is less than 10% but can be as high as 38% (average of 9.3% ± 7.7% $\sigma$). Source area samples are the same as those originally used for the Fe grain chemistry [*Darby*, 2003] and consist of tills, outwash deposits, fluvial sediments, and shallow shelf deposits (<50 m water depth for most) or channel bottom sediments in the Canadian Islands. See Figure 1 for source area abbreviations.

[b]Two or more nearby (<200 km) samples were combined or averaged.

[c]Only 4–45 $\mu$m analyzed.

the central Arctic. The lower concentrations could not be easily seen from the bridge of an icebreaker, especially after snowfalls. Once snows began covering the pack ice in late August (less than halfway through the expedition), only very heavy concentrations of dirty ice could be spotted from upturned ice block in the ships' wake. Yet little was found for nearly the entire cruise track across the Chukchi Borderland and the Mendeleev Ridge areas before snow cover hindered spotting dirty ice. Not until late August after initial snowfalls was dirty ice spotted

**Table 1.** (continued)

| | MR GS870817-G3 | North Alaska 82-APB-10 | North Alaska 72-AJT-30/41[b] | Chukchi Sea SI689-009 | Chukchi Sea TT020-020 | Chukchi Sea TT020-052 | Chukchi Sea 94BC01 | BS NW063-009 |
|---|---|---|---|---|---|---|---|---|
| Minerals | | | | | | | | |
| Quartz | 46.2 | 33.8 | 38.0 | 32.0 | 27.1 | 33.6 | 21.4 | 31.4 |
| Kspar (ordered microcline) | 2.2 | 0.7 | 0.5 | 1.5 | 2.5 | 2.0 | 1.5 | 2.1 |
| Kspar (intermediate) | 2.1 | 1.1 | 0.9 | 0.2 | 0.0 | 0.0 | 0.0 | 2.6 |
| Kspar (Sanidine) | 0.5 | 0.1 | 0.0 | 1.2 | 0.7 | 0.0 | 1.6 | 0.1 |
| Kspar (orthoclase) | 0.9 | 0.8 | 0.8 | 1.9 | 2.1 | 1.2 | 0.7 | 3.0 |
| Kspar (anorthoclase) | 0.6 | 0.0 | 0.0 | 2.6 | 1.6 | 0.4 | 0.1 | 6.2 |
| Plag (Albite) | 2.9 | 4.3 | 3.9 | 7.3 | 5.6 | 6.8 | 5.4 | 8.1 |
| Plag (oligoclase) | 1.2 | 1.1 | 0.9 | 4.0 | 3.7 | 3.2 | 3.2 | 3.0 |
| Plag (Andesine) | 0.0 | 0.0 | 0.0 | 0.0 | 0.0 | 0.0 | 0.0 | 2.9 |
| Plag (Labradorite) | 0.2 | 0.0 | 0.0 | 3.4 | 4.3 | 3.1 | 2.8 | 1.3 |
| Plag (Bytownite) | 0.0 | 0.0 | 0.0 | 1.3 | 0.8 | 0.1 | 0.0 | 1.1 |
| Plag (Anorthite) | 0.7 | 0.0 | 0.1 | 0.1 | 2.9 | 2.3 | 0.1 | 1.9 |
| Calcite | 4.7 | 3.3 | 14.5 | 0.0 | 0.0 | 0.0 | 0.0 | 0.0 |
| Calcite (Mg-rich) | 0.0 | 0.2 | 0.2 | 0.4 | 0.0 | 0.0 | 0.0 | 0.0 |
| Dolomite | 14.6 | 4.0 | 5.3 | 0.6 | 0.8 | 1.6 | 1.2 | 0.2 |
| Amph. (Ferrot.) | 0.7 | 0.0 | 0.0 | 1.3 | 1.1 | 0.8 | 0.0 | 1.8 |
| Pyroxene (diopside) | 0.1 | 0.0 | 0.0 | 0.3 | 0.7 | 0.8 | 0.0 | 0.2 |
| Magnetite | 0.2 | 0.0 | 0.1 | 0.4 | 0.0 | 0.0 | 0.0 | 0.3 |
| Maghemite | 0.0 | 0.7 | 0.1 | 0.0 | 0.0 | 0.0 | 0.0 | 0.1 |
| Non-clays | 77.8 | 50.1 | 65.4 | 58.6 | 54.0 | 55.9 | 38.0 | 66.4 |
| | | | | | | | | |
| Kaolinite (disordered) | 0.0 | 1.3 | 0.8 | 1.2 | 2.0 | 0.4 | 1.0 | 1.9 |
| Kaolinite (dry branch) | 0.0 | 0.1 | 0.0 | 0.0 | 0.0 | 0.5 | 0.2 | 0.0 |
| Smectite (Na) | 0.0 | 2.1 | 1.4 | 0.0 | 0.0 | 0.0 | 0.3 | 0.0 |
| Smectite (Ca) | 0.0 | 3.0 | 1.3 | 0.0 | 0.0 | 0.0 | 2.3 | 0.0 |
| Smectite (hectorite) | 2.7 | 3.6 | 2.5 | 1.9 | 0.9 | 2.1 | 5.0 | 0.0 |
| Smectite (Fe) | 0.0 | 1.4 | 0.6 | 3.4 | 6.3 | 1.9 | 3.3 | 1.6 |
| Illite (1Md) | 3.6 | 6.2 | 4.8 | 6.2 | 2.5 | 10.4 | 14.4 | 6.9 |
| Illite (R > 1; 70–80%I) | 2.0 | 5.8 | 4.5 | 3.3 | 0.0 | 1.8 | 3.1 | 0.0 |
| Illite (RM30) | 2.1 | 2.8 | 1.1 | 1.5 | 2.4 | 0.9 | 0.8 | 1.9 |
| Biotite | 0.0 | 0.2 | 0.0 | 0.2 | 1.1 | 0.0 | 1.2 | 0.1 |
| Chlorite (Fe) | 4.9 | 4.9 | 5.6 | 4.9 | 6.7 | 10.5 | 11.1 | 3.3 |
| Chlorite (Mg) | 0.6 | 1.4 | 1.2 | 0.9 | 2.8 | 1.0 | 1.0 | 2.3 |
| Muscovite | 6.4 | 13.7 | 10.3 | 14.7 | 20.3 | 14.6 | 17.1 | 14.3 |
| Vermiculite | 0.0 | 3.4 | 0.5 | 3.1 | 1.1 | 0.0 | 1.1 | 1.3 |
| | | | | | | | | |
| Summed rescaled clays | | | | | | | | |
| Illite | 63.2 | 57.5 | 59.8 | 62.7 | 57.0 | 62.9 | 59.0 | 69.0 |
| Chlorite | 24.7 | 12.6 | 19.7 | 14.1 | 20.6 | 26.2 | 19.6 | 16.6 |
| Smectite | 12.1 | 27.1 | 18.2 | 20.2 | 18.1 | 8.9 | 19.4 | 8.6 |
| Kaolinite | 0.0 | 2.8 | 2.3 | 3.0 | 4.3 | 2.1 | 2.0 | 5.8 |
| | | | | | | | | |
| <2 $\mu$m filter transfers | | | | | | | | |
| Illite | | 70.0 | | | | | 64.5 | |
| Chlorite | | 16.0 | | | | | 11 | |
| Smectite | | 3.5 | | | | | 15.5 | |
| Kaolinite | | 10.5 | | | | | 9 | |
| | | | | | | | | |
| Difference RJ versus <2 $\mu$m | | | | | | | | |
| Illite | | 12.5 | | | | | 5.5 | |
| Chlorite | | 3.4 | | | | | 8.6 | |
| Smectite | | 23.6 | | | | | 3.9 | |
| Kaolinite | | 7.7 | | | | | 7.0 | |

and sampled. Then two extensive bands of dirty ice were encountered on the Alpha Ridge near 84°N and 151°W over a distance of 148 km along the ship's track (sites H3-3 to H3-5, Figure 1) and again closer to the North Pole (a 300 km path including sites H3-7 to H3-10). A similar but more extensive band of dirty ice was encountered during the LOMROG expedition where heavy concentrations of dirty ice were spotted for nearly six consecutive days in almost continuous patches near 87°N in a near E-W trend extending 775 km (from 82.2° N, 9.9°E to 86.5°N, 53.0°W, near sites L1-L6, Figure 1). The total areal extent of these dirty ice patches and thus the total sediment load they transport is difficult to determine without satellite or aerial mapping, and this is hindered by the snow cover. These patches of dirty ice must be larger than what we could observe to either side of the ship's track (~500 m). Unless we were just incredibly lucky to encounter these patches of dirty ice, the probability of our doing so during each expedition is small enough to indicate that the extent of dirty ice was much larger than

**Table 1.** (continued)

| | ESS NW063-039GB | ESS NW063-55 | ESS NW063-64 | ESS NW063-90 | Indigirka R. IK93[b] | Laptev Sea NW063-173 | Ob R. OB67 | Yenisey R. YR93[b] |
|---|---|---|---|---|---|---|---|---|
| Minerals | | | | | | | | |
| Quartz | 27.1 | 31.1 | 28.9 | 20.4 | 28.0 | 23.6 | 29.7 | 18.0 |
| Kspar (ordered microcline) | 1.2 | 1.1 | 2.3 | 3.0 | 3.0 | 4.0 | 3.1 | 3.8 |
| Kspar (intermediate) | 2.0 | 3.2 | 1.8 | 0.6 | 1.4 | 5.4 | 2.7 | 2.6 |
| Kspar (Sanidine) | 1.4 | 0.4 | 1.2 | 1.4 | 1.6 | 2.0 | 1.4 | 0.5 |
| Kspar (orthoclase) | 3.0 | 3.7 | 1.5 | 1.8 | 1.4 | 2.9 | 0.5 | 0.0 |
| Kspar (anorthoclase) | 2.7 | 2.1 | 1.6 | 1.1 | 1.4 | 2.0 | 2.3 | 3.1 |
| Plag (Albite) | 7.7 | 12.3 | 11.7 | 7.8 | 11.6 | 9.9 | 7.1 | 6.9 |
| Plag (oligoclase) | 3.8 | 5.1 | 5.1 | 4.2 | 4.9 | 6.5 | 3.9 | 3.9 |
| Plag (Andesine) | 1.1 | 0.0 | 0.0 | 0.0 | 0.3 | 0.0 | 0.5 | 0.0 |
| Plag (Labradorite) | 1.0 | 0.1 | 0.8 | 0.1 | 0.7 | 2.9 | 0.1 | 6.9 |
| Plag (Bytownite) | 0.0 | 0.8 | 0.7 | 0.0 | 0.3 | 0.8 | 0.0 | 3.4 |
| Plag (Anorthite) | 1.3 | 1.8 | 1.3 | 0.8 | 1.0 | 1.0 | 0.8 | 1.6 |
| Calcite | 0.0 | 0.0 | 0.0 | 0.0 | 0.0 | 0.0 | 0.0 | 0.0 |
| Calcite (Mg-rich) | 0.0 | 0.0 | 0.0 | 0.0 | 0.0 | 0.0 | 0.0 | 0.0 |
| Dolomite | 0.0 | 0.1 | 0.1 | 0.0 | 0.2 | 0.1 | 0.1 | 0.0 |
| Amph. (Ferrot.) | 0.8 | 0.4 | 0.0 | 0.0 | 0.4 | 1.1 | 0.8 | 1.5 |
| Pyroxene (diopside) | 0.0 | 0.0 | 0.0 | 0.0 | 0.0 | 1.4 | 0.0 | 3.7 |
| Magnetite | 0.0 | 0.0 | 0.0 | 0.0 | 0.0 | 0.3 | 0.2 | 0.6 |
| Maghemite | 0.0 | 0.0 | 0.0 | 0.0 | 0.0 | 0.0 | 0.0 | 1.6 |
| Non-clays | 53.1 | 62.2 | 57.0 | 41.2 | 56.2 | 63.9 | 53.2 | 58.0 |
| Kaolinite (disordered) | 2.3 | 1.0 | 2.1 | 1.8 | 1.4 | 1.9 | 2.6 | 2.0 |
| Kaolinite (dry branch) | 0.0 | 0.0 | 0.0 | 0.0 | 0.0 | 0.0 | 0.0 | 0.0 |
| Smectite (Na) | 0.0 | 0.0 | 0.0 | 0.7 | 0.0 | 0.0 | 0.0 | 0.0 |
| Smectite (Ca) | 1.1 | 0.0 | 0.0 | 2.4 | 0.0 | 0.0 | 2.3 | 0.0 |
| Smectite (hectorite) | 4.1 | 2.3 | 3.0 | 5.2 | 2.4 | 3.5 | 5.9 | 5.1 |
| Smectite (Fe) | 3.6 | 2.8 | 3.4 | 4.7 | 4.0 | 4.3 | 8.0 | 6.1 |
| Illite (1Md) | 12.1 | 5.8 | 8.0 | 10.8 | 9.2 | 10.6 | 7.4 | 11.9 |
| Illite (R > 1; 70–80%I) | 0.0 | 0.6 | 1.6 | 3.4 | 2.4 | 1.4 | 3.6 | 0.0 |
| Illite (RM30) | 0.3 | 1.4 | 1.5 | 3.0 | 0.2 | 0.0 | 1.3 | 1.3 |
| Biotite | 0.0 | 0.0 | 0.8 | 0.8 | 0.6 | 0.7 | 0.5 | 0.8 |
| Chlorite (Fe) | 4.9 | 9.2 | 7.7 | 8.0 | 6.9 | 4.0 | 2.4 | 4.4 |
| Chlorite (Mg) | 1.0 | 0.7 | 1.0 | 1.4 | 0.9 | 1.1 | 1.2 | 0.9 |
| Muscovite | 16.0 | 13.7 | 14.2 | 14.8 | 13.8 | 6.6 | 11.5 | 6.9 |
| Vermiculite | 1.4 | 0.3 | 0.0 | 1.8 | 1.9 | 2.0 | 0.0 | 2.5 |
| Summed rescaled clays | | | | | | | | |
| Illite | 60.7 | 56.9 | 60.3 | 55.8 | 60.0 | 53.5 | 52.2 | 49.8 |
| Chlorite | 12.6 | 26.2 | 20.1 | 16.0 | 17.8 | 14.1 | 7.7 | 12.7 |
| Smectite | 21.8 | 14.3 | 14.8 | 25.2 | 19.0 | 27.1 | 34.6 | 32.7 |
| Kaolinite | 4.9 | 2.6 | 4.8 | 3.1 | 3.2 | 5.3 | 5.5 | 4.9 |
| <2 $\mu$m filter transfers | | | | | | | | |
| Illite | | 74.5 | | | 71 | 61.5 | 51 | 30.5 |
| Chlorite | | 20 | | | 17 | 14.5 | 9.5 | 11.5 |
| Smectite | | 2 | | | 3 | 12 | 29 | 48 |
| Kaolinite | | 3.5 | | | 9 | 12.5 | 10.5 | 10 |
| Difference RJ versus <2 $\mu$m | | | | | | | | |
| Illite | | 17.6 | | | 11.0 | 8.0 | 1.2 | 19.3 |
| Chlorite | | 6.2 | | | 0.8 | 0.4 | 1.8 | 1.2 |
| Smectite | | 12.3 | | | 16.0 | 15.1 | 5.6 | 15.3 |
| Kaolinite | | 0.9 | | | 5.8 | 7.2 | 5.0 | 5.1 |

the area covered by the ship's track. Using the length of the ship's track and half this distance in the normal direction, we obtain first-order estimates of the area of each dirty floe that range from 11,000 km$^2$ for the Alpha Ridge floes (H3-1 to H3-6) and 45,000 km$^2$ for the Lomonosov Ridge floes (H3-7 to H3-11) to about 300,000 km$^2$ for the LOMROG floes, or about the same area as the entrainment event in the eastern Laptev Sea in 1994/1995 [*Eicken et al.*, 2000]. The more or less continuous nature of the dirty ice suggests a single entrainment event for each of the three transects of dirty ice encountered in the central Arctic during the two expeditions, but there is no way to confirm this. For perspective, 300,000 km$^2$ is only about 3% of the central Arctic Ocean [*Jakobsson*, 2002]. Because of the much higher sediment concentrations encountered during the HOTRAX and LOMROG expeditions, there is a very good possibility that these are the largest Arctic sea ice entrainment events ever recorded with sediment loads estimated at 7 kg m$^{-2}$ in places and averaging 1.4 ± 2 kg m$^{-2}$. Thus

**Table 1.** (continued)

| | West Franz Josef Is. NP94-25PGC7 | West Franz Josef Is. NP94-41SC1 | East Svalbard NP94-40GC2 | East Svalbard NP94-38SC2 | Dirty Ice Samples | | | |
|---|---|---|---|---|---|---|---|---|
| | | | | | L1 | L2 | L3 | L4A |
| Minerals | | | | | | | | |
| Quartz | 24.0 | 26.3 | 24.9 | 24.4 | 20.0 | 20.7 | 16.7 | 19.0 |
| Kspar (ordered microcline) | 1.8 | 2.7 | 4.8 | 1.7 | 0.5 | 0.6 | 0.9 | 4.0 |
| Kspar (intermediate) | 0.0 | 0.0 | 1.6 | 0.0 | 5.0 | 5.2 | 3.1 | 0.6 |
| Kspar (Sanidine) | 0.6 | 1.6 | 0.7 | 1.2 | 0.6 | 0.6 | 1.4 | 1.4 |
| Kspar (orthoclase) | 0.0 | 0.3 | 0.6 | 0.0 | 2.7 | 2.8 | 2.5 | 0.0 |
| Kspar (anorthoclase) | 2.4 | 2.7 | 3.5 | 2.4 | 0.8 | 0.9 | 1.7 | 5.6 |
| Plag (Albite) | 5.3 | 3.6 | 4.7 | 5.1 | 8.8 | 8.7 | 6.8 | 6.3 |
| Plag (oligoclase) | 2.4 | 2.2 | 2.9 | 1.8 | 4.6 | 4.4 | 4.5 | 3.0 |
| Plag (Andesine) | 0.0 | 0.3 | 0.0 | 0.0 | 0.3 | 0.2 | 0.8 | 0.0 |
| Plag (Labradorite) | 0.0 | 0.0 | 0.2 | 0.1 | 0.0 | 1.7 | 0.0 | 2.2 |
| Plag (Bytownite) | 0.5 | 0.0 | 0.3 | 0.0 | 1.9 | 3.3 | 1.1 | 0.0 |
| Plag (Anorthite) | 0.1 | 0.7 | 0.5 | 0.3 | 0.0 | 0.0 | 0.2 | 1.2 |
| Calcite | 0.0 | 9.3 | 11.1 | 2.9 | 0.0 | 0.0 | 0.0 | 0.0 |
| Calcite (Mg-rich) | 0.0 | 0.0 | 0.0 | 0.0 | 0.0 | 0.0 | 12.4 | 0.8 |
| Dolomite | 0.1 | 4.4 | 4.4 | 1.7 | 0.0 | 0.0 | 0.0 | 1.2 |
| Amph. (Ferrot.) | 0.5 | 1.5 | 1.9 | 1.1 | 0.0 | 0.0 | 0.6 | 4.3 |
| Pyroxene (diopside) | 0.0 | 0.0 | 0.5 | 0.0 | 0.9 | 1.4 | 0.0 | 1.3 |
| Magnetite | 0.0 | 0.0 | 0.0 | 0.0 | 0.2 | 0.0 | 0.2 | 0.0 |
| Maghemite | 0.0 | 0.0 | 0.6 | 0.0 | 1.3 | 0.0 | 1.9 | 0.0 |
| Non-clays | 37.7 | 55.7 | 63.2 | 42.8 | 47.6 | 50.5 | 54.9 | 51.1 |
| Kaolinite (disordered) | 7.9 | 5.9 | 3.9 | 6.7 | 4.9 | 3.5 | 0.0 | 0.0 |
| Kaolinite (dry branch) | 0.0 | 0.1 | 0.1 | 1.1 | 0.0 | 0.0 | 0.0 | 0.0 |
| Smectite (Na) | 0.0 | 0.0 | 0.0 | 0.0 | 0.1 | 0.0 | 0.0 | 0.0 |
| Smectite (Ca) | 0.5 | 0.0 | 0.0 | 1.7 | 4.3 | 3.4 | 0.0 | 0.0 |
| Smectite (hectorite) | 2.0 | 0.0 | 0.0 | 0.8 | 7.5 | 6.2 | 7.8 | 10.4 |
| Smectite (Fe) | 5.2 | 4.2 | 2.3 | 2.8 | 5.2 | 6.4 | 5.4 | 0.0 |
| Illite (1Md) | 16.4 | 14.4 | 12.7 | 15.3 | 5.9 | 5.2 | 5.2 | 0.0 |
| Illite (R > 1; 70–80%I) | 4.7 | 1.5 | 0.0 | 2.7 | 3.4 | 1.8 | 0.5 | 0.0 |
| Illite (RM30) | 2.3 | 2.5 | 1.0 | 3.8 | 0.0 | 0.0 | 0.2 | 4.3 |
| Biotite | 0.0 | 0.0 | 1.4 | 0.0 | 0.9 | 0.0 | 2.3 | 6.3 |
| Chlorite (Fe) | 6.0 | 4.3 | 5.1 | 6.0 | 2.1 | 2.6 | 6.1 | 16.9 |
| Chlorite (Mg) | 1.1 | 0.0 | 1.2 | 1.6 | 1.1 | 1.4 | 0.2 | 0.0 |
| Muscovite | 13.5 | 9.4 | 7.5 | 13.0 | 10.0 | 9.9 | 6.0 | 11.0 |
| Vermiculite | 2.5 | 1.9 | 1.6 | 1.6 | 7.0 | 9.1 | 11.4 | 0.0 |
| Summed rescaled clays | | | | | | | | |
| Illite | 59.4 | 62.7 | 61.4 | 60.9 | 38.5 | 34.1 | 31.5 | 44.3 |
| Chlorite | 11.4 | 9.8 | 17.1 | 13.3 | 6.1 | 8.1 | 14.0 | 34.4 |
| Smectite | 16.4 | 13.9 | 10.6 | 12.1 | 46.0 | 50.7 | 54.4 | 21.3 |
| Kaolinite | 12.7 | 13.6 | 10.9 | 13.7 | 9.4 | 7.1 | 0.0 | 0 |
| <2 $\mu$m filter transfers | | | | | | | | |
| Illite | | | | | 50.5 | 38 | 44 | 54.5 |
| Chlorite | | | | | 14 | 9 | 15 | 15.7 |
| Smectite | | | | | 24 | 44.3 | 27 | 21.3 |
| Kaolinite | | | | | 12 | 8.7 | 14 | 8.8 |
| Difference RJ versus <2 $\mu$m | | | | | | | | |
| Illite | | | | | 12.0 | 3.9 | 12.5 | 10.2 |
| Chlorite | | | | | 7.9 | 0.9 | 1.0 | 18.7 |
| Smectite | | | | | 22.0 | 6.4 | 27.4 | 0.0 |
| Kaolinite | | | | | 2.6 | 1.6 | 14.0 | 8.8 |

estimates for the largest of these events (LOMROG floes) is up to $4 \times 10^8$ t or about 20 times earlier estimates of a probable suspension freezing event in 1994/19995 near the New Siberian Islands (east Laptev Sea) of $18.5 \times 10^6$ t [*Eicken et al.*, 2000].

[12] Several of the dirty ice floes sampled during the HOTRAX and LOMROG expeditions in the central Arctic and the area north of Fram Strait had similar characteristics. Most dirty ice occurred in patches of up to several hundred square meters (Figures 2a and 2b). Both concentrations of nearly ice-free sediment 2–10 cm thick and pellets scattered throughout the ice were encountered at each site (Figures 2c and 2d). One site had direct evidence of anchor ice in that articulated mollusk shells (Figures 2d and 2e) and sea weeds were found (Figure 2f). The mollusk shell is in ice with scattered pellets (1–3 mm) of sediment and larger clumps of sediment attached to the shell. If this was plucked directly from the seafloor, most of the sediment must have been remobilized during a previous melt season. Melt pond concentrations that cover a few square meters occur either as

**Table 1.** (continued)

| | Dirty Ice Samples | | | | | | |
|---|---|---|---|---|---|---|---|
| | L5 | H1-6 | H3-5 | H3-8[b] | H3-9 | H3-10 | H3-11 |
| Minerals | | | | | | | |
| Quartz | 18.3 | 24.2 | 26.6 | 23.4 | 23.5 | 25.8 | 22.4 |
| Kspar (ordered microcline) | 4.2 | 0.0 | 0.8 | 0.9 | 3.6 | 4.1 | 1.8 |
| Kspar (intermediate) | 0.0 | 3.2 | 3.2 | 4.4 | 1.7 | 1.4 | 4.4 |
| Kspar (Sanidine) | 2.1 | 0.5 | 0.8 | 0.9 | 0.6 | 0.2 | 0.0 |
| Kspar (orthoclase) | 0.0 | 1.5 | 2.0 | 1.3 | 0.5 | 2.8 | 1.5 |
| Kspar (anorthoclase) | 7.6 | 0.0 | 0.0 | 2.0 | 3.1 | 2.5 | 0.8 |
| Plag (Albite) | 6.2 | 11.6 | 12.8 | 12.9 | 8.8 | 8.4 | 9.1 |
| Plag (oligoclase) | 2.9 | 3.8 | 4.1 | 1.5 | 4.7 | 7.4 | 4.9 |
| Plag (Andesine) | 0.0 | 0.0 | 0.0 | 0.0 | 0.0 | 0.0 | 0.0 |
| Plag (Labradorite) | 1.1 | 0.0 | 0.0 | 0.5 | 1.0 | 0.5 | 1.8 |
| Plag (Bytownite) | 0.0 | 0.0 | 0.7 | 1.1 | 0.0 | 0.0 | 0.0 |
| Plag (Anorthite) | 0.7 | 0.5 | 0.0 | 0.0 | 1.7 | 1.3 | 0.1 |
| Calcite | 0.0 | 0.0 | 0.0 | 0.0 | 0.0 | 0.0 | 0.0 |
| Calcite (Mg-rich) | 0.4 | 0.0 | 0.0 | 0.1 | 0.0 | 0.0 | 0.0 |
| Dolomite | 1.2 | 0.4 | 0.1 | 0.2 | 0.0 | 0.1 | 0.1 |
| Amph. (Ferrot.) | 3.9 | 0.1 | 0.0 | 0.5 | 0.4 | 0.0 | 0.9 |
| Pyroxene (diopside) | 1.6 | 0.0 | 0.0 | 0.1 | 0.0 | 0.3 | 0.0 |
| Magnetite | 0.3 | 0.0 | 0.0 | 0.0 | 0.0 | 0.0 | 0.0 |
| Maghemite | 0.0 | 1.7 | 1.0 | 0.0 | 0.0 | 0.0 | 0.0 |
| Non-clays | 50.7 | 47.6 | 52.2 | 49.7 | 49.7 | 54.9 | 47.8 |
| Kaolinite (disordered) | 0.0 | 1.5 | 1.3 | 1.3 | 2.1 | 1.1 | 0.0 |
| Kaolinite (dry branch) | 0.0 | 0.0 | 0.0 | 0.0 | 0.0 | 0.6 | 0.0 |
| Smectite (Na) | 0.0 | 1.6 | 0.0 | 0.0 | 0.0 | 0.0 | 0.0 |
| Smectite (Ca) | 0.0 | 1.5 | 2.0 | 0.0 | 0.0 | 0.0 | 0.0 |
| Smectite (hectorite) | 8.6 | 7.7 | 5.1 | 3.2 | 4.7 | 5.2 | 0.0 |
| Smectite (Fe) | 0.0 | 0.1 | 1.4 | 1.9 | 1.7 | 3.0 | 5.4 |
| Illite (1Md) | 0.0 | 4.8 | 5.2 | 12.4 | 13.5 | 12.3 | 9.1 |
| Illite (R > 1; 70–80%I) | 0.0 | 5.7 | 4.7 | 2.0 | 0.0 | 0.0 | 5.2 |
| Illite (RM30) | 2.2 | 1.3 | 1.4 | 1.3 | 1.3 | 0.1 | 2.1 |
| Biotite | 6.2 | 0.9 | 0.9 | 0.9 | 1.6 | 0.4 | 0.1 |
| Chlorite (Fe) | 19.4 | 5.9 | 5.4 | 6.8 | 6.9 | 6.3 | 8.4 |
| Chlorite (Mg) | 1.0 | 1.2 | 1.2 | 1.8 | 0.4 | 0.0 | 1.5 |
| Muscovite | 11.0 | 16.5 | 15.4 | 15.0 | 16.1 | 14.9 | 15.5 |
| Vermiculite | 0.9 | 3.8 | 3.8 | 3.8 | 2.0 | 1.2 | 4.8 |
| Summed rescaled clays | | | | | | | |
| Illite | 39.3 | 55.7 | 57.9 | 62.8 | 64.6 | 61.4 | 61.6 |
| Chlorite | 41.4 | 13.6 | 13.8 | 17.0 | 14.5 | 14.0 | 18.9 |
| Smectite | 19.3 | 28.0 | 25.7 | 17.6 | 16.7 | 20.8 | 19.5 |
| Kaolinite | 0 | 2.8 | 2.7 | 2.5 | 4.2 | 3.8 | 0.0 |
| <2 $\mu$m filter transfers | | | | | | | |
| Illite | 54.8 | 65.5 | 70 | | | | |
| Chlorite | 12.5 | 17.5 | 19 | | | | |
| Smectite | 18.8 | 8 | 2 | | | | |
| Kaolinite | 14 | 9 | 9 | | | | |
| Difference RJ versus <2 $\mu$m | | | | | | | |
| Illite | 15.5 | 9.8 | 12.1 | | | | |
| Chlorite | 28.9 | 3.9 | 5.2 | | | | |
| Smectite | 0.5 | 20.0 | 23.7 | | | | |
| Kaolinite | 14 | 6.2 | 6.3 | | | | |

a continuous sediment layer up to 1–2 cm thick or small patches of sediment at the bottom of the ponds at each site (Figures 2e and 2f). There is no conclusive determination as to whether the thick accumulations of sediment were the result of concentration in melt ponds or original seafloor sediment entrapped in anchor ice. All of the thick sediment concentrations covered more than 5–10 $m^2$ (Figure 3). This is slightly larger than the average melt pond but melt ponds can be this large and cannot be ruled out. Many of the sediment concentrations were on and in ice that had been thrust into non-parallel attitudes, probably during previous year's pressure ridge formation (Figures 3c and 3d). All of the highly concentrated sediment in dirty ice occurred in multiyear ice as evidenced by the rough surface of the ice with local relief of nearly a meter and abundant pressure ridges. Based on the occurrence of the shells with only scattered sediment pellets instead of a thick layer of sediment and the multiyear nature of the floes, we suspect that the 2–10 cm thick concentrations observed during HOTRAX and LOMROG were melt pond deposits.

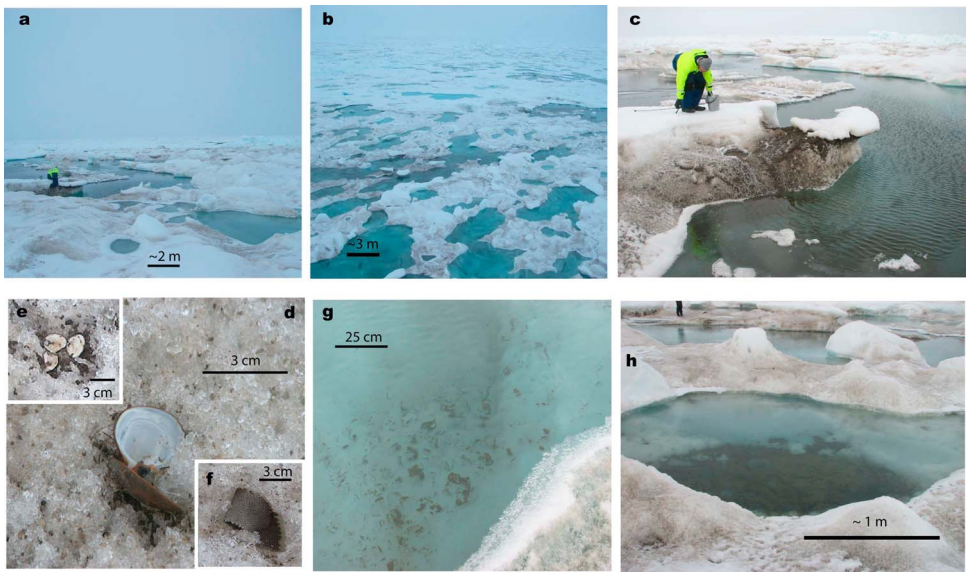


**Figure 2.** Photos of dirty ice at LOMROG expedition site L4. (a) Extent of dirty ice and melt ponds (20 August 2007); (b) oblique air photo showing the widespread nature of the sediment; (c) thickness of sediment layer is ~10 cm with about 10–20 cm of fresh snow above; (d) both valves of a mollusk shell, probably *Yoldia* genus, a shallow water mollusk; (e) several shells of the same genus as in Figure 2d from nearby; (f) fragment of a seaweed; (g) low concentration of sediment in a melt pond; and (h) heavy concentration of sediment in a melt pond.

[13] None of the dirty ice samples contained sediment coarser than 211 $\mu$m (H3-5) and most samples were finer than 60 $\mu$m (coarsest 95 percentile of the size distribution; Figure 4). The coarsest size in the one sampled floe with direct evidence of an anchor ice origin, i.e., the presence of shells, is only 80 $\mu$m. The mean size of all the dirty ice samples from both HOTRAX and LOMROG is 17 ± 22 $\mu$m and the maximum mean size is 94 $\mu$m (H3-5 and L5). The average of the coarsest 95 percentile in all dirty ice samples is 53 ± 50 $\mu$m.

### 3.2. Sources of Dirty Ice: Fe Grain Fingerprinting

[14] The EPMA fingerprinting of Fe oxide mineral grains has proven to be a reliable provenance tool in many studies,

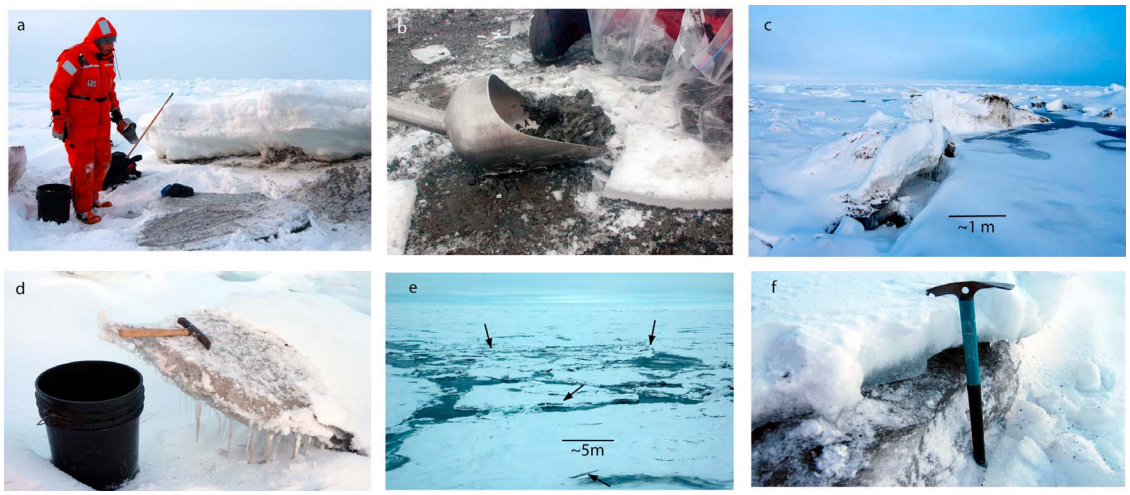


**Figure 3.** Photos of dirty ice from the HOTRAX expedition. (a) The 3–5 cm thick layer of sediment at site H3-7 (6 September 2005); (b) scoop used to collect sediment from 3 to 5 cm thick layer at site H3-5 (30 August 2005); (c) dirty ice on a pressure ridge at site H3-2 (29 August 2005); (d) sediment in pressure ridge at site H3-7; (e) oblique air photo showing lateral extent of dirty ice at site H3-3 with arrows pointing to heaviest concentrations (30 August 2005); (f) sediment in pressure ridge at site H3-6 (31 August 2005).

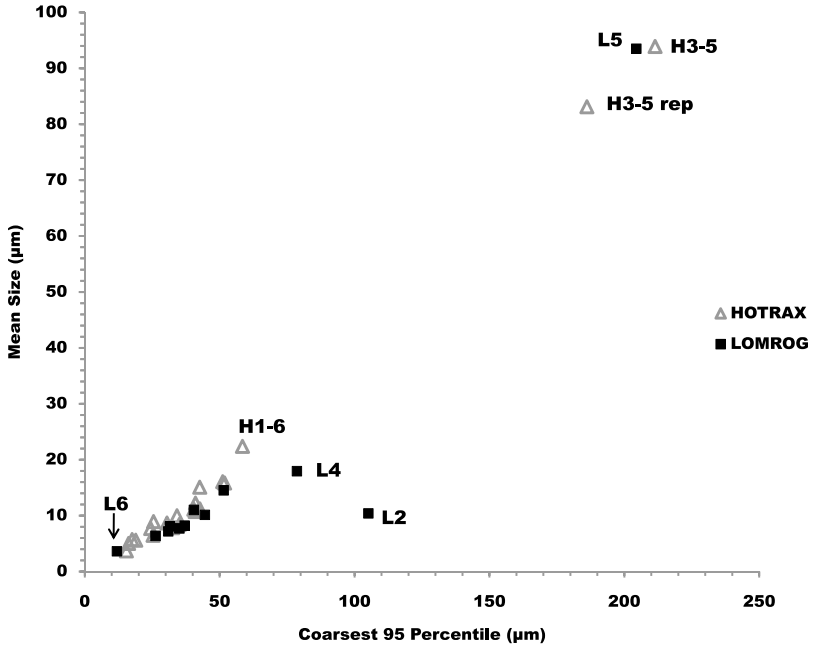


**Figure 4.** Texture of bulk dirty ice samples. Note the cluster of most samples with sediment less than about 100 $\mu$m including L4 containing the shells. The replicate analyses on H3-5 were made on sub-samples from the same sample site.

providing precise source determinations for individual detrital grains in each sample [*Darby and Bischof*, 1996, 2004; *Darby*, 1998, 2003, 2008; *Darby et al.*, 2001, 2002; *Darby and Zimmerman*, 2008; *Andrews et al.*, 2009]. Unlike any other provenance technique, numbers of grains can be quickly matched to potential sources to determine multiple sources contributing to a sample. A minimum of 5 grains must be matched to a particular source for a viable provenance determination [*Darby*, 2003]. Nearly half of the dirty ice sample sites contained adequate numbers of Fe grains for this threshold level (11/24). Only these samples will be discussed for Fe grain source determinations. The two dirty ice sample sites from offshore Alaska in the Beaufort Sea both indicated a Bering Strait source inferred to be from the Bering Sea or southern Chukchi Sea near Bering Strait (Figure 5). This is in contrast to several dirty ice samples collected between 1971 and 1995 just a few hundred kilometers east of these 2005 samples that showed a dominant Canadian source, primarily from the Banks Island area [*Darby*, 2003]. There were also significant amounts of Laptev Sea and Ob River grains in about two-thirds of these earlier samples. Even dirty ice samples collected in 1994 and 1996 from the Chukchi Sea west of the 2005 HOTRAX sites were matched to Banks Island area sources (including the shelves along Amundsen Gulf and McClure Strait) with one of these floes also containing Fe grains from the Laptev Sea [*Darby*, 2003]. Thus the 2005 samples off northern Alaska have a different provenance than previous dirty ice samples from this area.

[15] Eight of the nine central Arctic sampling sites (78%) matched to sources in the northern Canadian Islands, at least in part. Only one dirty ice sample matched only to a Russian source (H3-9) but two others matched to secondary Russian sources (H3-5 and L4). An earlier study of the Arctic Ocean Section expedition (AOS) dirty sea ice samples collected in 1994 showed only one of these four dirty AOS floes was from northern Canadian sources, with the others all from Russian Siberian sources, particularly the Laptev Sea [*Darby*, 2003]. Thus there is a significant difference in the proportion of Russian sources matched in older floes (1971–1995) and the 2005–2007 samples. There is a possibility that these floes sampled during the AOS94 were part of the entrainment event reported by *Eicken et al.* [2000] because they sourced to approximately the same area of the East Laptev Sea and were sampled later in the same year along the Trans Polar Drift (TPD). Thus variations in sources occur from year to year probably as a function of the Arctic Oscillation and the resulting change in the position of the TPD [*Proshutinsky and Johnson*, 1997; *Rigor et al.*, 2002; *Darby et al.*, 2006].

[16] Three of the eleven 2005/2007 dirty ice samples sourced to more than one area and two of these (H3-5 and L4) contained Russian and North American Fe grains (Figure 5). This is similar to the 1971–1995 dirty ice samples where five of seven multisource floes contained both Russian and North American Fe grains [*Darby*, 2003]. The proportion of multisource dirty ice samples from any source combination is only slightly smaller in 2005–2007 as compared to samples from 1971 to 1995 (27 versus 39%, respectively).

[17] Because of the large volume of sediment recovered during the LOMROG dirty ice sampling, replicate samples were prepared, analyzed and matched as if they were different samples. The results show that while the weighted percent varies with the number of total grains analyzed, for the most part, the results are fairly consistent especially for the dominant source area (Figure 5). Secondary sources in L4 and L5 showed greater variability among subsamples and this might be due to the fact that these subsamples were collected as much as 200 m from one another. The total of

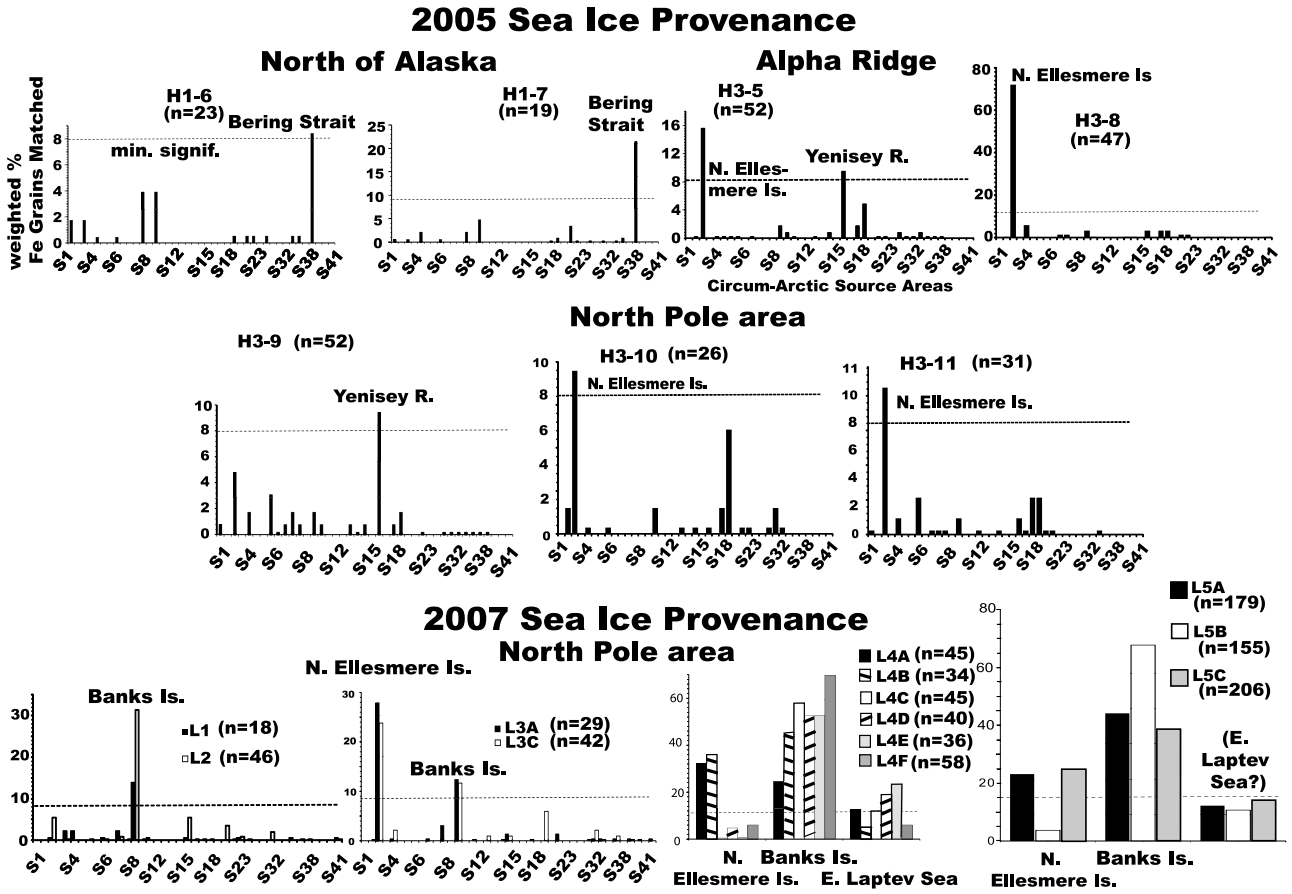


**Figure 5.** Sources for dirty ice samples based on Fe grain chemical matches to the circum-Arctic source database. S1 trough S41 are designated source areas [*Darby*, 2003]. Significant sources are labeled. N is the total number of Fe grains matched to all sources in each sample. Multiple sub-samples are shown in L3, L4, and L5. All sub-samples were collected from the same floe but several meters distance from each other and as such were treated as separate samples but show essentially the same sources for each floe. Only the three sources of the six subsamples in L4 with at least one subsample above the minimum significance level are shown. The same for L5 but the E. Laptev Sea source contribution is shown because it is close to the number of matched Fe grains required for minimal significance for this source. The minimum significance level is determined from tests discussed previously [*Darby*, 2003] and essentially these are 8–10% of the total grains matched for any particular sample; thus this minimum can vary slightly with the total number of grains matched but is generally between 8 and 15 weighted percent, only exceeding 10 weighted percent for grain numbers above 100 (dashed lines).

all matched grains in L4 sub-samples is 258 grains and for the three sub-samples in L5 the total is 540. These are large enough to provide statistically significant results and show that the same dominant sources (Banks Island for L4 and L5; N. Ellesmere Island for L3) are identified for the combined totals as for the individual sub-samples.

### 3.3. Sources Based on Drift Back Trajectories

[18] The back trajectories for the HOTRAX samples collected in June 2005 (H1-6/7 in Figure 1) indicate that the BG is rather large and robust during the years prior to 2005 under the influence of a mostly neutral to slightly negative Arctic Oscillation index. While there are no drift buoys in the Chukchi Sea that intersect these sample sites off northern Alaska, the Alaskan Coastal Current would bring ice from the Bering Strait area to very close to these sites [*Darby et al.*, 2009].

[19] All of the back trajectories for the central Arctic dirty ice samples (both HOTRAX H3-series and LOMROG L-series sample sites) indicate a drift path from the eastern Laptev Sea that could easily intersect with a robust BG (Figure 1). Given the variance in the actual drift paths and the monthly averaged drift (Figure 1), both the North American and Laptev sources provided by the Fe grain matches are easily reconciled. One particular buoy demonstrates the mingling of the BG and TPD. It began its drift near Banks Island in September 2003 and by September 2006 it was within the TPD at that time off the East Siberian Sea and 951 km from the North Pole (Figure 1). This buoy was about one year of drift distance from the 2007 LOMROG dirty ice locations when it stopped reporting. Thus while the back trajectories indicate the ice floes all originated near the eastern Laptev Sea, dirty floes from northern Canada drifting in the BG could easily mingle with these

Russian floes that probably had little or no sediment. Thus the Fe grain fingerprinting indicated the source of sediment, but not necessarily the origin of the bulk of the ice.

[20] H3-5, the ice floe that sourced to northern Ellesmere Is and the Yenisey River areas using Fe grain fingerprinting, is consistent with drift paths near the convergence of the TPD and BG. The drift in the southern Kara Sea near the mouth of the Ob and Yenisey Rivers is eastward toward Vilkitski Strait and into the Laptev Sea where the back trajectories indicate the source is located for these floes. The floes then drift north where they can mingle with floes originating anywhere in the North American coastal regions such as northern Ellesmere Island that become incorporated into the clockwise circulation of the BG. A similar drift history is inferred for L4, with similar sources as in H3-5. The buoy drift from the northern Laptev Sea to the LOMROG sample sites required two years according to drift buoys. Another year or two would be required for ice to drift to the northern Laptev Sea from the southern Kara Sea. Ice from northern Ellesmere Island would require several years to drift around the BG and then feed into the TPD. Alternatively there is an east-west divergence in ice drift near this source [e.g., *Rigor et al.*, 2002, Figures 4 and 9] and ice could drift directly north and east toward the H3-10/11 sample sites depending on which side of the divergence the floes begin.

### 3.4. Circum-Arctic Mineralogy

[21] Clay mineralogy, heavy mineral suites, trace elements, lithic grain counts, and isotopes have been used for ice-rafted detritus (IRD) provenance [*Wahsner et al.*, 1999; *Hemming et al.*, 2002; *Krylov et al.*, 2008; *Immonen et al.*, 2009; *Darby and Bischof*, 1996]. Of these, the most commonly used tool in the Arctic has been clay mineralogy [*Stein et al.*, 1994, 2004; *Vogt et al.*, 2001]. Clay minerals have the advantage of being abundant in dirty ice samples that are mostly very fine-grained. Like any proxy they have drawbacks as well. Clay minerals, especially the smectite group are size dependant and special care must be taken when separating the <2 $\mu$m fraction used for oriented XRD studies so that the sample is completely disaggregated and that the finest components containing most of the smectite are not enhanced at the surface of the XRD mount [*Gibbs*, 1965]. Even small errors in either of these preparation steps can result in large differences of more than 10–20% in the absolute smectite abundance. Expansion of smectite clays is also a source of abundance errors and care must be taken to insure complete expansion by ethylene glycol. Problems can also arise with the degree of orientation in the XRD mounts. In an attempt to avoid most of these problems, we used the entire <45 $\mu$m wet-sieve fraction and random mounts. Besides avoiding the size segregation issues, this has an important advantage over the oriented XRD mounts in that all of the hkl lattice indices can be determined so that different varieties of smectite and other clay minerals can be identified. These <45 $\mu$m XRD results are difficult to compare to the <2 $\mu$m oriented mounts because some of the illite and included muscovite occur in the >2 $\mu$m size fractions. Thus, this mineral along with chlorite, which also occurs in the >2 $\mu$m fractions, tend to be enhanced in our XRD results using the <45 $\mu$m size fraction.

[22] The clay minerals, rescaled to 100% indicate that illite is the most abundant Arctic Ocean clay mineral (Table 1) as was shown long ago [*Berry and Johns*, 1966; *Carroll*, 1970; *Darby*, 1975]. More germane to sea ice provenance is the abundance of smectite, which has been used as an indicator of a Kara Sea or west Laptev Sea source due to the abundance of smectite there from the weathering of volcanic rocks on the nearby Taymyr Peninsula and watersheds of the Ob and Yenisey Rivers.

[23] Studies of clay mineralogy for the circum-Arctic shelves have focused on the Russian side and few studies of the clay mineralogy of the North American Arctic shelves exist [*Stein et al.*, 2002, and references therein; *Stein*, 2008]. We selected samples with sufficient material in the <45 $\mu$m fraction for XRD analyses from the large circum-Arctic sample database used for Fe grain chemical analyses. We selected 29 samples that were representative of a good geographic coverage of the entire Arctic and focused on areas commonly identified as sources for the Fe-grain fingerprinting provenance. Many of these selected samples are from North American shelves or coastal sediments that are underrepresented in published clay and non-clay mineralogical data sets for provenance (Figure 1 and Table 1).

[24] Our circum-Arctic clay mineral data confirm earlier reports on these minerals [*Wahsner et al.*, 1999; *Stein et al.*, 2002, and references therein] and fill-in several gaps. Expandable clays (smectite and Mg vermiculite) appear to be more widely distributed around the Arctic than previously reported, ranging from ~33–35% in the Ob and Yenisey rivers to 1% in northern Greenland (GL30), and a mean of 18.5% for all source samples (rescaled clays in Table 1). Besides the elevated regional values of smectite in the southern Kara Sea, primarily the Ob and Yenisey River mouths, there are values of >20% in many locations around the Arctic Ocean and total expandable clays are comparable to the southern Kara Sea in some North American sites (Figure 1 and Table 1). Elevated amounts of calcic and sodic varieties of smectite as well as the expansive clay vermiculite are more typical of the North American Arctic, whereas hectorite and ferruginous smectite phases are more abundant in the Russian Arctic, but it is doubtful that the differences are adequate to distinguish these sources.

[25] Illite (including mica) concentrations ranged from 82% in northern Greenland (GL30) to a low of 36% in Victoria Island, with a mean of 60% (Table 1). Illite is nearly ubiquitous in the Arctic, with typical weight percents of >50% of the clays. It is also the dominant clay mineral in Arctic Ocean sediments [*Darby*, 1975; *Nürnberg et al.*, 1994, 1995; *Stein et al.*, 1994; *Wahsner et al.*, 1999]. Kaolinite concentrations are fairly low around the Arctic, with elevated values near or around Ellef Ringnes Island as well as Spitsbergen and Franz Josef Land. Kaolinite ranges from zero to 19% with a mean of 5% of the rescaled clays. Chlorite ranges from >25% (TT020–052, NW063–55, and Victoria Island) to less than 10–13% in Axel Heiberg Island (R390), Ob R., and Franz Josef Land with a mean of 17%.

[26] Quartz is the most abundant non-clay mineral in the <45 $\mu$m fraction followed by variable amounts of several other minerals such as K-feldspar, plagioclase, calcite and dolomite. The carbonate minerals have been used to indicate a Canadian source due to the abundance of mostly dolomites in the Victoria Island area. There are relatively high amounts

of both calcite and dolomite in several other circum-Arctic areas as well, but mostly North American sources and not Russian (Table 1). The highest calcite concentration is on Bathurst Island (14%; 95BJB0003), with other elevated values found in Northern Alaska, Ellesmere Island, and the northern Barents Sea. Dolomite was very high in samples from Victoria Island (Stefansson Island and Storkerson Peninsula; 60%) with 32% in northern Ellesmere Island (Otto Fjord), but was virtually non-existent in the Russian sources. Victoria Island has the highest concentration of amphibole (3%; Storkerson Peninsula). Also, elevated amphibole concentrations were found in the Russian Arctic (1.5–1.7% in the Yenisey River and Spitsbergen).

[27] Bulk sample (<45 $\mu$m) quartz values in the source samples range from <5% (Victoria Island) to 46% (Mackenzie R. delta) with a mean of >27%. The coastal areas from northern Greenland to Alaska generally have high quartz contents. The Russian half of the Arctic is typified by high (>25%) total feldspar (K-Feldspar + plagioclase feldspar), while totals of <15% and often half this value are more typical of the North American region (Table 1). This can be seen in the individual feldspar types as well, with the highest K-feldspar values being found in Laptev Sea sediments (16%; NW063–173), with nearby samples exceeding 8–9% (Yenisey River and East Siberian Sea). Plagioclase feldspar is similar, with the highest values of ~23% found in the Yenisey River and >20% in Laptev and East Siberian Seas.

### 3.5. Dirty Ice Mineralogy

[28] The bulk mineralogy is fairly consistent for the HOTRAX and LOMROG dirty ice samples, but different from most source samples (Table 1). Quartz concentrations are generally 4–10% lower than most source samples. Average high Mg calcite concentrations are low, but much higher than in the circum-Arctic source sample set (due to elevated value in one sample; L3). The clay mineralogy of most sea ice samples contain elevated levels of expandable clays (smectite + vermiculite) relative to most source samples. From the summed and rescaled clay percentages plotted in Figure 1, it is apparent that the HOTRAX samples all contain much higher illite than the LOMROG samples. Cluster analysis of all samples was used to find close mineral compositions between dirty ice and source samples, but the sea ice samples either cluster with each other or with several sources making it difficult to determine a source (Figure 6). For example, HOTRAX samples H1-6, H3-5, 8, and 11 cluster together with 9 different source samples from Alaska to the Ob River. None of the other sea ice samples clustered with any source samples.

[29] Using summed and rescaled values of clay mineral types, there are also several source samples in the circum-Arctic data set that match dirty ice samples, especially the HOTRAX dirty ice samples (Figure 1). Yet none of these matches have the same proportion of varieties of each clay mineral group. A key fact in the clay mineral provenance of the dirty ice samples analyzed here is the low chlorite content of the southern Kara Sea (Ob and Yenisey Rivers) samples while all of the dirty sea ice samples except L1 and L2 contain higher chlorite values despite high smectite contents (Figure 1). L1and L2 appear more similar to Canadian sources like Ellef Ringnes Island, while L3, L4, and L5 are most similar to Victoria Island (Figure 1). L1, L2, and L3 contain higher smectite values than any source area sample (Table 1). All of the HOTRAX dirty ice samples have similar rescaled clay mineral contents but differ in individual mineral percents (Table 1). Comparing the rescaled values in Figure 1, the HOTRAX samples could easily match to northern Alaska, Bering Strait, Chukchi, East Siberian Sea, and the Ob and Yenisey rivers. Yet there are individual mineral differences in each of these areas that nullify any match. If you allow for enough variance to match these ice samples to any of these sources, there is no unique match and they overlap with several sources in composition. In fact, despite their different illite contents relative to HOTRAX, all of the LOMROG samples could easily match to similar sources including Banks/Victoria Island, northern Ellesmere Island, and northern Alaska.

## 4. Discussion

### 4.1. Dirty Ice Characteristics and Sources: Implications for the Entrainment Process

[30] Despite the wide range in the coarsest particles (95 percentile) in the dirty ice samples from 12 to 211 $\mu$m, all of the samples were finer than the maximum particle size for sea ice entrainment previously suggested as less than 250 $\mu$m [*Reimnitz et al.*, 1993b, 1998; *Nürnberg et al.*, 1994; *Eicken et al.*, 2005]. Because anchor ice entrains whatever sediment is available on the seafloor, if coarser particles are present they should be entrained. The lack of sediment coarser than 250 $\mu$m however, suggests that such coarse particles cannot be used as criteria for anchor ice. Because the mean and coarsest particle sizes cluster near the finer sizes and include the one sample with shells (L4) that is most surely due to anchor ice, using the presence of coarse grains alone to distinguish anchor ice and suspension freezing is problematic (Figure 4). Principal component analyses of the <45 $\mu$m size analyses of these same dirty ice samples indicates a coarse silt-size component that was interpreted to represent anchor ice [*Darby et al.*, 2009]. Perhaps the 250 $\mu$m size limit, which was really intended to distinguish sea ice from glacial iceberg IRD, is too large for distinguishing anchor ice and suspension freezing. Thus the presence of sediment coarser than about 100–150 $\mu$m might indicate an anchor ice over suspension freezing when glacial ice can be excluded, but the absence of such large grains alone cannot be used to indicate suspension freezing. This is primarily due to the fact that many shallow shelves in the Arctic probably lack coarse sediment and anchor ice would only entrain fine sediment.

[31] The lack of material coarser than 211 $\mu$m in the HOTRAX and LOMROG dirty ice samples however suggest that the entrainment did not occur in the beach or nearshore zone where wave activity during open water conditions would most always produce sandy sediment of this and coarser sizes. All but one of the LOMROG samples and four of the HOTRAX samples contained sediment coarser than 30 $\mu$m, and three of these HOTRAX samples were from off Alaska where all of the dirty ice floes contained low sediment concentrations and might be due to suspension freezing. Five of the HOTRAX samples and four of the LOMROG samples contain sediment coarser than 50 $\mu$m, including the one with the shells (L4). This coupled with the finding of a coarse silt component [*Darby*

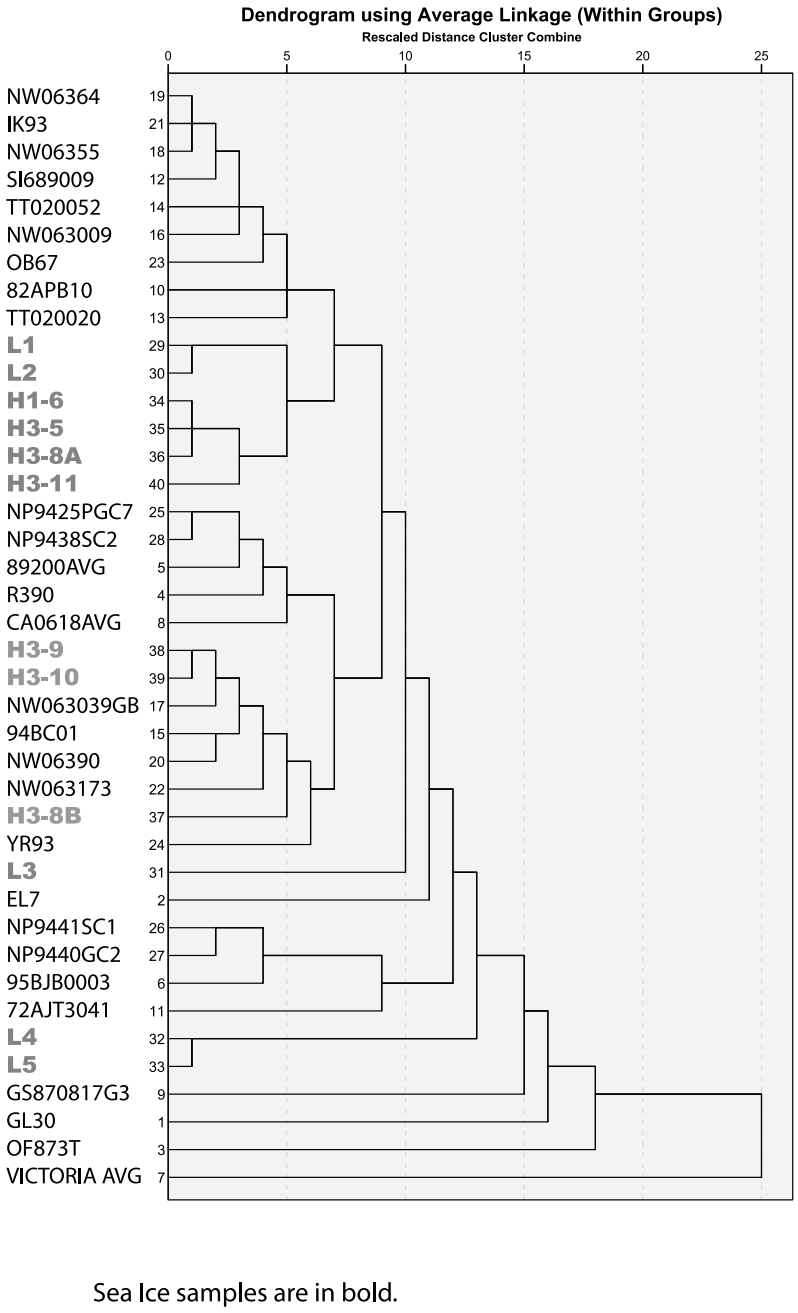


**Figure 6.** Dendrogram of hierarchical cluster analysis using average linkage between groups of the bulk mineral content (<45 $\mu$m) from XRD and RockJock abundance calculations. The sea ice samples are in bold, while the other samples are potential source samples. The sea ice samples either cluster with other sea ice samples or with several source samples equally so that specific sources could not be determined.

*et al.*, 2009] might suggest that suspension freezing generally involves sediment less than 30–60 $\mu$m at the 95 percentile of the coarsest sizes and anchor ice entrains coarser particles than this. Size alone is an inadequate indicator of the two entrainment processes.

[32] The Fe grain fingerprinting indicates that most of the 2005 and 2007 dirty ice floes originated in the shallow coastal North American sector. The floes originating in northern Canada would most likely become entrained in the BG for three to as many as 20 or more years depending on the number of rotations they make before merging with the TPD and drifting toward Fram Strait. Although such multiple rotations in the BG are less likely today with the extensive melting experienced in the last decade [e.g., *Kwok et al.*, 2009]. The drift trajectories based on drift buoys show that the BG was fairly large in diameter and was close to the TPD during the two to three years prior to 2005 (Figure 1). This is conducive for floes to move out of the BG and into the TPD within three years.

[33] Samples H1-6 and H1-7 near Alaska are from the Bering Strait according to Fe grain matches and this agrees with the surface drift in this area where the Alaska Coastal

Current moves north along the west coast of Alaska transporting Bering Strait ice to the H1-6 site aided by offshore eddies once the floes reach the northern coast of Alaska (Figure 1) [*Pickart*, 2004; *Pickart et al.*, 2005]. The low concentration of sediment in all floes off northern Alaska and the coarsest particles less than 60 $\mu$m (mean size <30 $\mu$m) suggest a suspension freezing origin.

[34] The central Arctic dirty ice samples sourced to Canada based on Fe grain fingerprinting (H3-5, H3-8, H3-10, H3-11 and all LOMROG samples) probably were initially drifting in the BG and then merged into the TPD. The net drift for these samples are indicated by the dashed yellow path (Figure 1) while those samples matched to Russian sources (H3-5 and H3-9) drifted east along the coast, through Vilkitski Strait past the Lena River before turning north near the New Siberian Islands as indicated by the net drift (red dashed line in Figure 1) and the buoy drift trajectories for the two years preceding the floes reached the sampling locations on the Alpha Ridge. This drift pattern has been documented for dirty sea ice floes in earlier studies [*Pfirman et al.*, 1997; *Wahsner et al.*, 1999; *Eicken et al.*, 2000; *Vogt and Knies*, 2008].

[35] Although values up to 70% smectite in the <2 $\mu$m fraction have been reported for the mouths of the Ob and Yenisey Rivers [*Wahsner et al.*, 1999], values above 25% are uncommon in sea ice samples [*Dethleff et al.*, 2000]. All of the 2005 HOTRAX dirty ice samples show less than 26% smectite (summed and rescaled to 100%) except for one sample, H1-6 at 28% smectite collected off Alaska (Table 1). All of the <45 $\mu$m XRD LOMROG sea ice samples show very high smectite values (46–54% of clay and mica rescaled to 100% in Table 1) and higher vermiculite than any of the source area samples, including the Ob and Yenisey Rivers. Thus neither the bulk mineralogy, nor clay mineralogy clearly indicate sources in the data set. Yet the summed and rescaled clay mineral percents shown in Figure 1 for the HOTRAX dirty ice samples could be linked to several possible source areas from Alaska to the Ob River, but none that have the exact same mix of clay mineral species (Table 1). The LOMROG dirty ice samples (L1–3) contain similar illite as the Victoria/Banks Island samples to which they all matched according to the Fe grain fingerprinting, but contained higher muscovite as well as much higher smectite and kaolinite than this source area (Table 1). These sources are tills from important Late Pleistocene ice streams from the Laurentide ice sheet outlet to the Arctic Ocean [*Stokes et al.*, 2005]. Thus large amounts of this sediment must have been transported west through McClure Strait and deposited on the Canadian shelves near Banks Island where it could be mixed with other sediments containing different fine-grained clays without changing the sand-size Fe grains. From here the sediment could be entrained by sea ice. Thus based on the Fe grain provenance and the drift patterns in place for the years preceding the sampling of the 2005/2007 dirty ice floes (Figure 1), the Banks Island area source for the LOMROG samples and the Canadian sources for the HOTRAX samples agrees with known drift patterns in this area.

[36] Flaw leads or polynya conditions occur throughout the circum-Arctic coastal areas and except for the Cape Bathurst Polynya near Banks Island are more common and more extensive in the Russian Arctic [*Hannah et al.*, 2009; *Stringer and Groves*, 1991; *Overland and Guest*, 1991; *Dmitrenko et al.*, 2005]. Thus the abundance of dirty ice from North America is unexpected if we assume that flaw leads and polynyas are the primary factor in sea ice entrainment. We can only be certain that one of these floes, L-4, is due to anchor ice, and this floe is sourced to the Banks Island area, probably the shallow (<60 m) areas around this island or fringing McClure Strait or Amundsen Gulf that coincide with the Cape Bathurst Polynya [*Arrigo and van Dijken*, 2004; *Barber and Massom*, 2007] (Figure 1). The presence of shells and seaweeds in the ice as well as the nearly 10 cm thick sediment concentration over more than 5–10 $m^2$ are the primary indicators of an anchor ice origin for this floe. In addition to the sites sampled in 2005/2007, nearly continuous sightings of similar heavy concentrations of dirty ice were observed along the three areas of sampling (Figure 1). We cannot be certain that all of these originated as anchor ice, but the amounts and thicknesses observed in many of them would be difficult to account for by melt-pond concentration of dilute dirty ice from suspension freezing. The dispersed nature of this form of sea ice entrainment would require much larger melt ponds than generally observed. In order to produce the thick sediment concentrations observed, sediment from an estimated area of more than 100–500 $m^2$ of low sediment concentration due to suspension freezing would have to flow into an area of about 5–10 $m^2$ to produce the thick concentrations observed for the dirty ice in 2005/2007. The slopes for such drainage just do not exist on the packice. Thus the high concentrations of sediment in the dirty ice floes observed in 2005/2007 were probably the result of anchor ice entrainment. Yet, *Reimnitz et al.* [1987] concluded that anchor ice only forms in sandy sediments where the particles are large enough to overcome buoyancy and drag effects as the ice grows and the ice can form in the interstitial pore spaces and thus entrain sediment to greater depths below the seafloor. We contend that there are insufficient observations to exclude the formation of anchor ice in silty sediments where the sediment cohesion and interstitial ice in the sediment pore space counters these lift effects until the ice is sufficiently thick to lift off large amounts of the bottom sediment. While only sandy sediments have thus far been observed to have anchor ice attached to the bottom, there is no reason to believe that the higher pore volumes in fine-grained silt and clay with up to 80%, which is more than twice that of sandy sediments, could not also support anchor ice.

[37] Some of the dirty floes suspected to be anchor ice are sourced to areas with rare or small flaw leads such as northern Ellesmere Island (Figure 5). If these floes are anchor ice, then the mechanism of initiating bottom water freezing in the absence of flaw leads during the winter needs to be explained. We are assuming that very little anchor ice will form in shallow water during the summer months due to the generally above freezing, open surface waters at this time. One scenario that does not require open water during the winter and the continuous advection of super-cooled water to the bottom is that of seed-ice formation. This scenario only requires the formation of ice within the bottom sediment at some time during the year, preferably in the fall or early winter before the pack ice forms so that bottom ice can grow all winter. If super-cooled seawater is not advected

to the bottom for ice initiation, then the flux of fresh groundwater from the continent through the underlying sediments might be the cause of ice formation because this fresh water would freeze at the ambient seawater temperatures during the late fall and winter (−1°C to −2°C [*Aagaard*, 1984; *Reimnitz et al.*, 1987]). Once ice forms in the sediment pore spaces it will provide a seed for further ice formation from seawater, which is at the freezing point. Unfortunately there is virtually no observation of groundwater flux into the Arctic Ocean so this process remains speculative.

[38] Another possibility for sediment entrainment is sediment frozen into the keels of sea ice pressure ridges as they become grounded. Pressure ridges can extend several meters below the pack ice and can become grounded or plough bottom sediment, although observations on this are very scarce to non-existent. There are no observations or studies of whether this process could entrain significant amounts of sediment although there have been speculation that it does [*Forbes and Taylor*, 1994, and references therein]. Unless the keels of such pressure ridges remain in contact for long periods of time to allow the ice to act as seed crystals and freeze pore water in the sediment, entrainment is unlikely. If ice is grounded for long periods in shallow water, there is the problem of whether it will become free before Spring melting occurs as open water could occur offshore of this ice, which could promote its melting before it can be incorporated in any ice pack drifting into the central Arctic [*Reimnitz et al.*, 1994]. Another problem is that the sediment will be overlain by several meters of sea ice and all of this has to melt in subsequent summers before this sediment can make its way to the surface of the pack ice where it can be observed and sampled.

[39] The near continuous occurrence of dirty ice over hundreds of kilometers suggests that the dirty ice was entrained and introduced into the ice drift at about the same time. If these dirty floes originated as anchor ice, this also needs explanation because only suspension freezing has been observed to produce such widespread events [*Eicken et al.*, 2000]. Anchor ice will become incorporated into the overlying packice only when it is sufficiently thick so that its buoyancy overcomes its attachment to the seafloor. There is no observation of anchor ice actually lifting off the bottom so we can only speculate that if the ice begins to grow under favorable conditions, that the conditions for ice growth should be fairly uniform for a particular coastal region regardless of whether the ice initiated due to groundwater flux into the offshore sediments or by seed crystals due to open water and convection of super cooled water to the bottom in the Fall. Thus the ice should reach a critical thickness at about the same time over rather large areas. The role of sudden events, such as Spring tides, internal waves, or currents in affecting this process has yet to be explored, but might also provide an explanation for near simultaneous lift-off of anchor ice.

### 4.2. Reworking of Sediment in Sea Ice

[40] The longer a floe is drifting, the greater the chance that it will merge with floes from other sources through the constant opening of leads and collision of floes forming pressure ridges [*Darby*, 2003]. When floes merge, the sediment can also mix due to summer melting and the flow of sediment into melt ponds. Based on the number of dirty sea ice samples containing multiple sources in this study and previous studies [*Darby*, 2003], a little more than a quarter to a third of floes result in mixing of entrained sediment. Of course there is another possibility that there are source areas as yet unsampled by us that contain sediment from multiple sources that would produce the results in Figure 5. Of the more than 450 circum-Arctic source samples we have never seen one with Fe grains that could be matched to more than one source above the minimum level of significance.

[41] Regardless of the Fe grain source, all of the dirty ice samples contained different mineral contents than the indicated or nearby source samples. Although for dirty ice samples with multiple Fe grain sources, a mix of two or more source samples combined with selective sorting of the clays could result in the measured clay mineral contents of these floes. None of the single-sourced Fe grain sources contained the same mix of clays or non-clays as any of the dirty ice samples, thus the sediment in these floes must have been altered during transport across the Arctic or the location of the actual entrainment was not analyzed for mineralogy. The fact that nearly all of the HOTRAX dirty ice samples contained a similar clay mineralogy suggests that the summer melting and meltwater flow into melt ponds as well as occasional partial drainage of these melt ponds into the ocean might be altering the clay mix. This might occur if certain sized clays are entrained by meltwater while others are not. Similarly, density and size differences in the non-clay fraction could cause hydraulic sorting as well. If so, this introduces another problem in the use of mineral abundances for sea ice provenance. This would not cause a change in the Fe grain composition because the Fe minerals are of similar size with densities above 4.5 and would respond similarly to hydraulic sorting.

## 5. Conclusions

[42] Anchor ice entrainment can be recognized in dirty ice by the presence of benthic shells or other particles much larger than 30–60 $\mu$m (95 percentile), and by sediment concentrations in layers of more than a few centimeters thick extending over an area of more than about 5–10 $m^2$. While the presence of benthic shells larger than 0.5–1 cm can be used alone to indicate anchor ice, the presence of sediment >30–60 $\mu$m should be used in conjunction with heavy concentrations over large areas (>5–10 $m^2$). Many of the dirty ice floes sampled as well as those observed but not sampled during the HOTRAX and LOMROG expeditions of 2005 and 2007, respectively, meet the criteria above for anchor ice. While suspension freezing is probably more widespread in the Arctic, anchor ice entrainment of bottom sediment accounts for much higher sediment concentrations in sea ice. The fact that so many dirty ice floes encountered during these two icebreaker expeditions contained heavy concentrations of sediment (avg. $1.4 \pm 2$ kg $m^{-2}$) of probable anchor ice origin suggests that this process is more common than previously thought and might rival suspension freezing for the total amount of sediment transported by ice in the Arctic today. If so, then our perceptions of where sea ice entrainment is likely to occur should include areas lacking extensive flaw leads or polynyas such as northern Canada.

[43] The pack ice is an even more dynamic environment for mixing of floes and entrained sediment than realized. More than a quarter of dirty ice floes analyzed in this study and by *Darby* [2003] contain multiple sources. The sediment in dirty floes is also reworked during the summer melt. It can move downward in cryoconite holes [*Reimnitz et al.*, 1993a] as well as flow into nearby melt ponds. Lateral transport of meltwater is probably limited due to the low gradient and lack of any appreciable slopes, but this short distance of movement along with occasional partial drainage of melt ponds, might be enough to hydraulically sort the sediment and change the abundance of some minerals. Future sampling of dirty ice floes should focus on sediment concentrations and the areal distribution of sediments. This and the presence of rare benthic shells and other biota are the only features that might distinguish anchor ice entrainment from suspension freezing.

[44] **Acknowledgments.** We thank the officers and crew of both the USCGC *Healy* and Swedish icebreaker *Oden* as well as the Swedish Polar Secretariat for their assistance in collecting the dirty ice samples. We also thank K. St. John and an anonymous reviewer for their helpful suggestions. Funding was provided by NSF grants OPP- 0612493 and OPP-0806857 to the lead author. M. Jakobsson's contribution was supported by the Swedish Research Council (VR), the Knut and Alice Wallenberg Foundation, and the Bert Bolin Centre for Climate Research at Stockholm University. I. Rigor's contribution was funded by grants from NASA, NOAA, NSF, and ONR.

## References

Aagaard, K. (1984), The Beaufort Undercurrent, in *The Alaskan Beaufort Sea: Ecosystems and Environments*, edited by P. W. Barnes et al., pp. 47–72, Academic, Orlando, Fla.

Andrews, J. T., D. Darby, D. Eberl, A. E. Jennings, M. Moros, and A. Ogilvie (2009), A robust, multisite Holocene history of drift ice off northern Iceland: Implications for North Atlantic climate, *Holocene*, *19*, 71–77, doi:10.1177/0959683608098953.

Arrigo, K. R., and G. L. van Dijken (2004), Annual cycles of sea ice and phytoplankton in Cape Bathurst polynya, southeastern Beaufort Sea, Canadian Arctic, *Geophys. Res. Lett.*, *31*, L08304, doi:10.1029/2003GL018978.

Barber, D. G., and R. A. Massom (2007), The role of sea ice in Arctic and Antarctic polynyas, in *Polynyas Windows to the World*, *Elsevier Oceanogr. Ser.*, vol. 74, edited by W. O. Smith Jr. and D. G. Barber, pp. 1–43, Elsevier, Amsterdam.

Barnes, P. W., E. Reimnitz, and D. Fox (1982), Ice rafting of fine-grained sediment, a sorting and transport mechanism, Beaufort Sea, Alaska, *J. Sediment. Petrol.*, *52*, 493–502.

Berry, R. W., and W. D. Johns (1966), Mineralogy of clay-sized fractions of some North Atlantic-Arctic ocean bottom sediments, *Geol. Soc. Am. Bull.*, *77*, 183–196, doi:10.1130/0016-7606(1966)77[183:MOTCFO]2.0.CO;2.

Biscaye, P. E. (1965), Mineralogy and sedimentation of recent deep-sea clay in Atlantic Ocean and adjacent seas and oceans, *Geol. Soc. Am. Bull.*, *76*, 803–832, doi:10.1130/0016-7606(1965)76[803:MASORD]2.0.CO;2.

Carroll, D. (1970), Clay minerals in Arctic Ocean sea-floor sediments, *J. Sediment. Petrol.*, *40*, 814–821.

Darby, D. A. (1975), Kaolinite and other clay minerals in Arctic Ocean sediment cores, *J. Sediment. Petrol.*, *45*, 272–279.

Darby, D. A. (1998), Mysterious iron-nickel-zinc spherules, *Can. J. Earth Sci.*, *35*, 23–29, doi:10.1139/cjes-35-1-23.

Darby, D. A. (2003), Sources of sediment found in sea ice from the western Arctic Ocean, new insights into processes of entrainment and drift patterns, *J. Geophys. Res.*, *108*(C8), 3257, doi:10.1029/2002JC001350.

Darby, D. A. (2008), Arctic perennial ice cover over the last 14 million years, *Paleoceanography*, *23*, PA1S07, doi:10.1029/2007PA001479.

Darby, D. A., and J. F. Bischof (1996), A statistical approach to source determinations of lithic and Fe-oxide grains: An example for the Alpha Ridge, Arctic Ocean, *J. Sediment. Res.*, *66*, 599–606.

Darby, D. A., and J. F. Bischof (2004), A Holocene record of changing Arctic ocean ice drift, analogous to the effects of the Arctic Oscillation, *Paleoceanography*, *19*, PA1027, doi:10.1029/2003PA000961.

Darby, D. A., and P. Zimmerman (2008), Ice-rafted detritus events in the Arctic during the last glacial interval and the timing of the Innuitian and Laurentide ice sheet calving events, *Polar Res.*, *27*, 114–127, doi:10.1111/j.1751-8369.2008.00057.x.

Darby, D., J. Bischof, G. Cutter, A. de Vernal, C. Hillaire-Marcel, G. Dwyer, J. McManus, L. Osterman, L. Polyak, and R. Poore (2001), New record of pronounced changes in Arctic Ocean circulation and climate, *Eos Trans. AGU*, *82*, 601, doi:10.1029/01EO00345.

Darby, D. A., J. F. Bischof, R. F. Spielhagen, S. A. Marshall, and S. W. Herman (2002), Arctic ice export events and their potential impact on global climate during the late Pleistocene, *Paleoceanography*, *17*(2), 1025, doi:10.1029/2001PA000639.

Darby, D. A., L. Polyak, and H. Bauch (2006), Past glacial and interglacial conditions in the Arctic Ocean and marginal seas, a review, *Prog. Oceanogr.*, *71*, 129–144, doi:10.1016/j.pocean.2006.09.009.

Darby, D. A., J. Ortiz, L. Polyak, S. Lund, M. Jakobsson, and R. A. Woodgate (2009), The role of currents and sea ice in both slowly deposited central Arctic and rapidly deposited Chukchi-Alaskan margin sediments, *Global Planet. Change*, *68*, 58–72, doi:10.1016/j.gloplacha.2009.02.007.

Dayton, P. K., G. A. Robillia, and A. L. Devries (1969), Anchor ice formation in McMurdo Sound Antarctica and its biological effects, *Science*, *163*, 273–274, doi:10.1126/science.163.3864.273.

Dethleff, D., and E. W. Kempema (2007), Langmuir circulation driving sediment entrainment into newly formed ice: Tank experiment results with application to nature (Lake Hattie, United States; Kara Sea, Siberia), *J. Geophys. Res.*, *112*, C02004, doi:10.1029/2005JC003259.

Dethleff, D., and G. Kuhlmann (2009), Entrainment of fine-grained surface deposits into new ice in the southwestern Kara Sea, Siberian Arctic, *Cont. Shelf Res.*, *29*, 691–701, doi:10.1016/j.csr.2008.11.009.

Dethleff, D., V. Rachold, M. Tintelnot, and M. Antonow (2000), Sea-ice transport of riverine particles from the Laptev Sea to Fram Strait based on clay mineral studies, *Int. J. Earth Sci.*, *89*, 496–502, doi:10.1007/s005310000109.

Dethleff, D., E. Kempema, R. Koch, and I. Chubarenko (2009), On the helical flow of Langmuir circulation–Approaching the process of suspension freezing, *Cold Reg. Sci. Technol.*, *56*, 50–57, doi:10.1016/j.coldregions.2008.10.002.

Dmitrenko, I. A., K. N. Tyshko, S. A. Kirillov, H. Eicken, J. A. Holemann, and H. Kassens (2005), Impact of flaw polynyas on the hydrography of the Laptev Sea, *Global Planet. Change*, *48*, 9–27, doi:10.1016/j.gloplacha.2004.12.016.

Eberl, D. D. (2003), User's guide to RockJock, a program for determining quantitative mineralogy from powder X-ray diffraction data, *U.S. Geol. Surv. Open File Rep.*, *03-78*, 56 pp.

Eicken, H., E. Reimnitz, V. Alexandrov, T. Martin, H. Kassens, and T. Viehoff (1997), Sea-ice processes in the Laptev Sea and their importance for sediment export, *Cont. Shelf Res.*, *17*, 205–233, doi:10.1016/S0278-4343(96)00024-6.

Eicken, H., J. Kolatschek, J. Freitag, F. Lindemann, H. Kassens, and I. Dmitrenko (2000), A key source area and constraints an entrainment for basin-scale sediment transport by Arctic sea ice, *Geophys. Res. Lett.*, *27*, 1919–1922, doi:10.1029/1999GL011132.

Eicken, H., R. Gradinger, A. Gaylord, A. Mahoney, I. Rigor, and H. Melling (2005), Sediment transport by sea ice in the Chukchi and Beaufort Seas: Increasing importance due to changing ice conditions?, *Deep Sea Res., Part II*, *52*, 3281–3302, doi:10.1016/j.dsr2.2005.10.006.

Forbes, D. L., and R. B. Taylor (1994), Ice in the shore zone and the geomorphology of cold coasts, *Prog. Phys. Geogr.*, *18*, 59–89, doi:10.1177/030913339401800104.

Gargett, A., J. Wells, A. E. Tejada-Martinez, and C. E. Grosch (2004), Langmuir supercells: A mechanism for sediment resuspension and transport in shallow seas, *Science*, *306*, 1925–1928, doi:10.1126/science.1100849.

Gibbs, R. J. (1965), Error due to segregation in quantitative clay mineral X-ray diffraction mounting techniques, *Am. Mineral.*, *50*(10), 741–751.

Hannah, C. G., F. Dupont, and M. Dunphy (2009), Polynyas and tidal currents in the Canadian Arctic Archipelago, *Arctic*, *62*, 83–95.

Hemming, S. R., T. O. Vorren, and J. Kleman (2002), Provinciality of ice rafting in the North Atlantic: Application of $^{40}Ar/^{39}Ar$ dating of individual ice rafted hornblende grains, *Quat. Int.*, *95–96*, 75–85, doi:10.1016/S1040-6182(02)00029-0.

Immonen, N., K. Strand, and S. Turunen (2009), Mineraological evidence of middle Miocene glacial ice in the central Arctic Ocean sediments, *Geophysica*, *45*, 59–67.

Jakobsson, M. (2002), Hypsometry and volume of the Arctic Ocean and its constituent seas, *Geochem. Geophys. Geosyst.*, *3*(5), 1028, doi:10.1029/2001GC000302.

Jakobsson, M., R. Macnab, L. Mayer, R. Anderson, M. Edwards, J. Hatzky, H. W. Schenke, and P. Johnson (2008), An improved bathymetric portrayal of the Arctic Ocean: Implications for ocean modeling and geolog-

ical, geophysical and oceanographic analyses, *Geophys. Res. Lett.*, *35*, L07602, doi:10.1029/2008GL033520.
Kempema, E. W., E. Reimnitz, and P. W. Barnes (1989), Sea ice sediment entrainment and rafting in the Arctic, *J. Sediment. Petrol.*, *59*, 308–317.
Kempema, E. W., E. Reimnitz, J. R. Clayton, and J. R. Payne (1993), Interactions of frazil and anchor ice with sedimentary particles in a flume, *Cold Reg. Sci. Technol.*, *21*, 137–149, doi:10.1016/0165-232X(93)90003-Q.
Krylov, A. A., I. A. Andreeva, C. Vogt, J. Backman, V. V. Krupskaya, G. E. Grikurov, K. Moran, and H. Shoji (2008), A shift in heavy and clay mineral provenance indicates a middle Miocene onset of a perennial sea ice cover in the Arctic Ocean, *Paleoceanography*, *23*, PA1S06, doi:10.1029/2007PA001497.
Kwok, R., G. F. Cunningham, M. Wensnahan, I. Rigor, H. J. Zwally, and D. Yi (2009), Thinning and volume loss of the Arctic Ocean sea ice cover: 2003–2008, *J. Geophys. Res.*, *114*, C07005, doi:10.1029/2009JC005312.
Maslanik, J., T. Agnew, M. R. Drinkwater, W. Emery, C. Fowler, R. Kwok, and A. Liu (1998), Summary of ice-motion mapping using passive microwave data: Report prepared for the Polar Data Advisory Group, *NSIDC Spec. Rep. 8*, 25 pp., Natl. Snow and Ice Data Cent., Boulder, Colo.
Nürnberg, D., I. Wollenburg, D. Dethleff, H. Eicken, H. Kassens, T. Letzig, E. Reimnitz, and J. Thiede (1994), Sediments in Arctic sea-ice: Implications for entrainment, transport and release, *Mar. Geol.*, *119*, 185–214, doi:10.1016/0025-3227(94)90181-3.
Nürnberg, D., M. A. Levitan, J. A. Pavlidis, and E. S. Shelekhova (1995), Distribution of clay minerals in surface sediments from the eastern Barents and south-western Kara seas, *Geol. Rundsch.*, *84*(3), 665–682, doi:10.1007/s005310050032.
Osterkamp, T. E., and J. P. Gosink (1984), Observations and analyses of sediment-laden sea ice, in *The Alaskan Beaufort Sea: Ecosystems and Environments*, edited by P. W. Barnes et al., pp. 73–93, Academic, Orlando, Fla.
Overland, J. E., and P. S. Guest (1991), The arctic snow and air-temperature budget over sea ice during winter, *J. Geophys. Res.*, *96*, 4651–4662, doi:10.1029/90JC02264.
Pfirman, S. L., R. Colony, D. Nürnberg, H. Eicken, and I. Rigor (1997), Reconstructing the origin and trajectory of drifting Arctic sea ice, *J. Geophys. Res.*, *102*, 12,575–12,586, doi:10.1029/96JC03980.
Pickart, R. S. (2004), Shelfbreak circulation in the Alaskan Beaufort Sea: Mean structure and variability, *J. Geophys. Res.*, *109*, C04024, doi:10.1029/2003JC001912.
Pickart, R. S., T. J. Weingartner, L. J. Pratt, S. Zimmermann, and D. J. Torres (2005), Flow of winter-transformed Pacific water into the Western Arctic, *Deep Sea Res., Part II*, *52*, 3175–3198, doi:10.1016/j.dsr2.2005.10.009.
Proshutinsky, A. Y., and M. A. Johnson (1997), Two circulation regimes of the wind-driven Arctic Ocean, *J. Geophys. Res.*, *102*, 12,493–12,514, doi:10.1029/97JC00738.
Reimnitz, E., and E. W. Kempema (1987), Field observations of slush ice generated during freeze-up in Arctic coastal waters, *Mar. Geol.*, *77*, 219–231, doi:10.1016/0025-3227(87)90113-7.
Reimnitz, E., E. W. Kempema, and P. W. Barnes (1987), Anchor ice, seabed freezing, and sediment dynamics in shallow arctic seas, *J. Geophys. Res.*, *92*, 14,671–14,678, doi:10.1029/JC092iC13p14671.
Reimnitz, E., L. Marincovich, M. McCormick, and W. M. Briggs (1992), Suspension freezing of bottom sediment and biota in the Northwest Passage and implications for Arctic Ocean sedimentation, *Can. J. Earth Sci.*, *29*, 693–703, doi:10.1139/e92-060.
Reimnitz, E., P. W. Barnes, and W. S. Weber (1993a), Particulate matter in pack ice of the Beaufort Gyre, *J. Glaciol.*, *39*, 186–198.
Reimnitz, E., J. R. Clayton, E. W. Kempema, J. R. Payne, and W. S. Weber (1993b), Interaction of rising frazil with suspended particles: tank experiments with applications to nature, *Cold Reg. Sci. Technol.*, *21*, 117–135, doi:10.1016/0165-232X(93)90002-P.
Reimnitz, E., D. Dethleff, and D. Nűrnberg (1994), Contrasts in Arctic shelf sea-ice regimes and some implications: Beaufort Sea versus Laptev Sea, *Mar. Geol.*, *119*, 215–225, doi:10.1016/0025-3227(94)90182-1.
Reimnitz, E., M. McCormick, J. Bischof, and D. A. Darby (1998), Comparing sea-ice sediment load with Beaufort Sea shelf deposits: Is entrainment selective?, *J. Sediment. Res.*, *68*, 777–787.
Rigor, I. G., and J. M. Wallace (2004), Variations in the age of Arctic sea-ice and summer sea-ice extent, *Geophys. Res. Lett.*, *31*, L09401, doi:10.1029/2004GL019492.
Rigor, I. G., J. M. Wallace, and R. L. Colony (2002), Response of sea ice to the Arctic oscillation, *J. Clim.*, *15*(18), 2648–2663, doi:10.1175/1520-0442(2002)015<2648:ROSITT>2.0.CO;2.
Stein, R. (2008), *Arctic Ocean Sediments: Processes, Proxies, and Paleoenvironment*, 592 pp., Elsevier, New York.
Stein, R., H. Grobe, and M. Wahsner (1994), Organic-carbon, carbonate, and clay mineral distributions in eastern central Arctic Ocean surface sediments, *Mar. Geol.*, *119*, 269–285, doi:10.1016/0025-3227(94)90185-6.
Stein, R., F. Niessen, D. Dittmers, M. Levitan, F. Schoster, J. Simstich, T. Steinke, and O. V. Stepanets (2002), Siberian River run-off and late Quaternary glaciation in the southern Kara Sea, Arctic Ocean: Preliminary results, *Polar Res.*, *21*, 315–322, doi:10.1111/j.1751-8369.2002.tb00086.x.
Stein, R., K. Dittmers, K. Fahl, M. Kraus, J. Matthiessen, F. Niessen, M. Pirrung, Y. Polyakova, F. Schoster, T. Steinke, and D. K. Futterer (2004), Arctic (palaeo) river discharge and environmental change: Evidence from the Holocene Kara Sea sedimentary record, *Quat. Sci. Rev.*, *23*, 1485–1511, doi:10.1016/j.quascirev.2003.12.004.
Stierle, A. P., and H. Eicken (2002), Sediment inclusions in Alaskan coastal sea ice: Spatial distribution, interannual variability, and entrainment requirements, *Arct. Antarct. Alp. Res.*, *34*, 465–476, doi:10.2307/1552205.
Stokes, C. R., C. D. Clark, D. A. Darby, and D. A. Hodgson (2005), Late Pleistocene ice export events into the Arctic Ocean from the M'Clure Strait Ice Stream, Canadian Arctic Archipelago, *Global Planet. Change*, *49*, 139–162, doi:10.1016/j.gloplacha.2005.06.001.
Stringer, W. J., and J. E. Groves (1991), Location and areal extent of polynyas in the Bering and Chukchi Seas, *Arctic*, *44*, 164–171.
Vogt, C., and J. Knies (2008), Sediment dynamics in the Eurasian Arctic Ocean during the last deglaciation: The clay mineral group smectite perspective, *Mar. Geol.*, *250*, 211–222, doi:10.1016/j.margeo.2008.01.006.
Vogt, C., J. Knies, R. F. Spielhagen, and R. Stein (2001), Detailed mineralogical evidence for two nearly identical glacial/deglacial cycles and Atlantic Water advection to the Arctic Ocean during the last 90,000 years, *Global Planet. Change*, *31*, 23–44, doi:10.1016/S0921-8181(01)00111-4.
Wahsner, M., C. Muller, R. Stein, G. Ivanov, M. Levitan, E. Shelekhova, and G. Tarasov (1999), Clay-mineral distribution in surface sediments of the Eurasian Arctic Ocean and continental margin as indicator for source areas and transport pathways: A synthesis, *Boreas*, *28*, 215–233, doi:10.1111/j.1502-3885.1999.tb00216.x.

D. A. Darby and W. B. Myers, Department of Ocean, Earth, and Atmospheric Sciences, Old Dominion University, 4600 Elkhorn Ave., Norfolk, VA 23529, USA. (ddarby@odu.edu)
M. Jakobsson, Department of Geological Sciences, Stockholm University, SE-106 91 Stockholm, Sweden.
I. Rigor, Applied Physics Laboratory, University of Washington, 1013 NE 40th St., Seattle, WA 98105, USA.